

Randolph Glacier Inventory – A Dataset of Global Glacier Outlines: Version 6.0

GLIMS Technical Report

RGI Consortium*, July 2017

* Members of the RGI Consortium are listed in section 1.5.

Table of Contents

1	Introduction	4
1.1	What is the RGI?	4
1.2	Version History	4
1.3	Data Distribution Policy	6
1.4	Data Sources.....	6
1.5	Dataset Reference	6
2	Definitions of the RGI Regions	8
3	Data Description	12
3.1	Technical Specifications	12
3.2	Data Fields and Hypsometry	12
3.3	Glacier Delineation.....	18
3.4	Quality Control	18
4	Revisions in RGI 6.0	19
4.1	Overview	19
4.2	Known Flaws.....	19
5	Description of Data Compilation by Region	20
5.1	REGION 1: Alaska.....	20
5.2	REGION 2: Western Canada and US.....	24
5.3	REGION 3: Arctic Canada North.....	26
5.4	REGION 4: Arctic Canada South	28
5.5	REGION 5: Greenland Periphery	30
5.6	REGION 6: Iceland	33
5.7	REGION 7: Svalbard	35
5.8	REGION 8: Scandinavia	38
5.9	REGION 9: Russian Arctic	40
5.10	REGION 10: North Asia.....	42
5.11	REGION 11: Central Europe.....	44
5.12	REGION 12: Caucasus and Middle East.....	46
5.13	REGION 13: Central Asia.....	48
5.14	REGION 14: South Asia West.....	51
5.15	REGION 15: South Asia East	53
5.16	REGION 16: Low Latitudes.....	55
5.17	REGION 17: Southern Andes	58
5.18	REGION 18: New Zealand	62
5.19	REGION 19: Antarctic and Subantarctic.....	63
6	Summary of Regional Glacier Counts and Areas	65
7	References	66

Randolph Glacier Inventory (RGI) – A Dataset of Global Glacier Outlines: Version 6.0

GLIMS Technical Report
RGI Consortium, July 2017

1 Introduction

1.1 What is the RGI?

The Randolph Glacier Inventory (RGI) is a globally complete inventory of glacier outlines. It is supplemental to the database compiled by the Global Land Ice Measurements from Space initiative (GLIMS). While GLIMS is a multi-temporal database with an extensive set of attributes, the RGI is intended to be a snapshot of the world's glaciers as they were near the beginning of the 21st century (although in fact its range of dates is still substantial). Production of the RGI was motivated by the preparation of the Fifth Assessment Report of the Intergovernmental Panel on Climate Change (IPCC AR5). The RGI was released initially with little documentation in view of the IPCC's tight deadlines during 2012. More documentation is provided in the current version of this Technical Report. The full content of the RGI has now been integrated into the database of GLIMS. However work remains to be done to make the RGI a downloadable subset of GLIMS, offering complete one-time coverage, version control and a standard set of attributes.

The RGI was not designed for the measurement of glacier-by-glacier rates of area change, for which the greatest possible accuracy in dating, delineation and georeferencing is essential. Many RGI outlines pass this test, but in general completeness of coverage has had higher priority. Rather, the strength of the RGI lies in the capacity it offers for handling many glaciers at once, for example for estimating glacier volumes and rates of elevation change at regional and global scales and for simulating cryospheric responses to climatic forcing.

In July 2014 development of the RGI became the responsibility of the Working Group on the Randolph Glacier Inventory and Infrastructure for Glacier Monitoring, a body of the International Association of Cryospheric Sciences (IACS). Its members are listed in Table 1.

1.2 Version History

Version 1.0 of the RGI was released in February 2012. It included a considerable number of unsubdivided ice bodies, which we refer to as glacier complexes, and a considerable number of nominal glaciers, which are glaciers for which only a location and an area are known; they are represented by circles of the appropriate area at the given location. An unofficial update of version 1.0 was provided in April 2012 to replace several regions that had topology errors and repeated polygons. Version 2.0, released in June 2012, eliminated a number of flaws and provided a uniform set of attributes for each glacier. Several outlines were improved, and a number of outlines were added in previously omitted regions. Version 2.0 also added shapefiles for its first-order and second-order regions.

Version 3.0 was an interim release representing the RGI as of 7 April 2013. It was the basis for the work of Gardner et al. (2013). The main improvements included identification of all tidewater basins, and separation of glacier complexes into glaciers in nearly all regions. Version 3.2, released in August 2013, included additional separation of glacier complexes into glaciers, and repairs of

some geometry errors. It is the basis for the scientific description and analysis of the RGI by Pfeffer et al. (2014).

Version 4.0 was released in December 2014. The most significant enhancement was the addition of topographic and hypsometric attributes for nearly all glaciers. These new attributes are described in detail below (section 3.2). Many glacier outlines were unchanged in version 4.0, but many more glaciers were assigned dates or date ranges, some names were added or corrected, and the inventory of Alaska was new. Remaining glacier complexes in Bolivia were subdivided, and nominal glaciers were added to correct omissions in the Greater Caucasus. A global grid of glacierized area with 0.5-degree resolution was added.

Version 5.0, released in July 2015, had new coverage of most of Asia (RGI regions 10, 13, 14 and 15), with some improved outlines elsewhere. Linkages to the Fluctuations of Glaciers database of the World Glacier Monitoring Service were provided for some glaciers with mass-balance measurements.

Version 6.0, released in July 2017, has improved coverage of the conterminous US (regions 02-05 and 02-06), Scandinavia (region 08) and Iran (region 12-2). In Scandinavia several hundred smaller glaciers have been added and most glaciers now have exact dates. The flag attributes *RGIFlag* and *GlacType* were reorganized. Surging codes have been added from Sevestre and Benn (2015).

Table 1 – IACS Working Group on the Randolph Inventory and Infrastructure for Glacier Monitoring

http://www.cryosphericosciences.org/wg_randGlacierInv.html

Co-chairs

Graham Cogley Trent University, Peterborough, Canada (gcogley@trentu.ca)
Regine Hock University of Alaska Fairbanks, USA (rehock@alaska.edu)

Members

Etienne Berthier CNRS-OMP-LEGOS, Toulouse, France
Andrew Bliss Colorado State University, USA
Tobias Bolch University of Zürich, Switzerland and Technische Universität Dresden, Germany
Koji Fujita University of Nagoya, Japan
Alex Gardner Jet Propulsion Laboratory, California Institute of Technology, USA
Matthias Huss University of Fribourg and ETH Zürich, Switzerland
Georg Kaser University of Innsbruck, Austria
Christian Kienholz University of Alaska Southeast, Juneau, USA
Anil Kulkarni Indian Institute of Science, Bangalore, India
Shiyin Liu State Key Laboratory of Cryospheric Sciences, Lanzhou, China
Christopher Nuth University of Oslo, Norway
Ben Marzeion University of Innsbruck, Austria
Takayuki Nuimura University of Nagoya, Japan
Frank Paul University of Zürich, Switzerland
Valentina Radić University of British Columbia, Canada
Bruce Raup National Snow and Ice Data Center, Boulder, USA
Akiko Sakai University of Nagoya, Japan
Donghui Shangguan Cold and Arid Regions Environmental & Engineering Research Institute, Lanzhou, China

1.3 Data Distribution Policy

The RGI may be used freely with due acknowledgement (by citing this note for technical details or Pfeffer et al. 2014 for scientific background). The inventory and this Technical Note can be downloaded from <http://www.glims.org/RGI/randolph60.html>.

1.4 Data Sources

The RGI is a combination of new and previously-published glacier outlines. New outlines were provided by the authors of this report, and by others in the glaciological community in response to requests for data on the GLIMS and Cryolist e-mail listservers. Publications describing regional inventories that were sources for the RGI are cited in Chapter 5 below, where updates of successive versions beyond version 1.0 are also described.

For version 1.0, we visualized the data in a geographic information system by overlaying outlines on modern satellite imagery, and assessed their quality relative to other available products. In several regions the outlines already in GLIMS were used for the RGI. Data from the World Glacier Inventory (WGI, http://nsidc.org/data/docs/noaa/g01130_glacier_inventory/; WGI, 1989) and the related WGI-XF (<http://people.trentu.ca/~gcogley/glaciology>; Cogley, 2009) were used for some nominal glaciers, mainly in the Pyrenees and in northern Asia. Where no other data were available we relied on data from the Digital Chart of the World (Danko, 1992).

1.5 Dataset Reference

Earlier versions of this technical note were referenced as Arendt et al. (various dates). The following form of reference is now recommended:

RGI Consortium, 2017, *Randolph Glacier Inventory (RGI) – A Dataset of Global Glacier Outlines: Version 6.0*. Technical Report, Global Land Ice Measurements from Space, Boulder, Colorado, USA. Digital Media. DOI: <https://doi.org/10.7265/N5-RGI-60>.

Members of the Randolph Consortium:

Arendt, A., A. Bliss, T. Bolch, J.G. Cogley, A.S. Gardner, J.-O. Hagen, R. Hock, M. Huss, G. Kaser, C. Kienholz, W.T. Pfeffer, G. Moholdt, F. Paul, V. Radić, L.M. Andreassen, S. Bajracharya, N.E. Barrand, M. Beedle, E. Berthier, R. Bhambri, I. Brown, E. Burgess, D. Burgess, F. Cawkwell, T. Chinn, L. Copland, B. Davies, H. De Angelis, G.A. Diolaiuti, E. Dolgova, L. Earl, K. Filbert, R. Forester, A.G. Fountain, H. Frey, B. Giffen, N. Glasser, W.Q. Guo, S. Gurney, W. Hagg, D. Hall, U.K. Haritashya, G. Hartmann, C. Helm, S. Herreid, M.J. Hoffman, I. Howat, G. Kapustin, N. Karimi, T. Khromova, M. König, J. Kohler, D. Krieger, S. Kutuzov, J. Landmann, I. Lavrentiev, R. LeBris, S.Y. Liu, R. Lo, J. Lund, W. Manley, R. Marti, F. Maussion, C. Mayer, E.S. Miles, X. Li, B. Menounos, A. Mercer, N. Mölg, P. Mool, G. Nosenko, A. Negrete, T. Nuimura, C. Nuth, R. Pettersson, A. Rabatel, A. Racoviteanu, R. Ranzi, P. Rastner, F. Rau, B. Raup, J. Rich, H. Rott, A. Sakai, C. Schneider, Y. Seliverstov, H. Sevestre, M. Sharp, O. Sigurðsson, C. Smiraglia, C. Stokes, R.G. Way, R. Wheate, S. Winsvold, G. Wolken, F. Wyatt, N. Zheltyhina.

The first 14 members, listed in alphabetical order, were responsible for the design and initial assembly of the RGI and for the necessary software development. The remaining authors, also listed

in alphabetical order, contributed essential data and in several cases assisted in compilation and checking. Although efforts have been made to trace the names of GLIMS contributors whose outlines are now in the RGI, it is possible that some have been missed. We also do not include the name of every contributor to the WGI or WGI-XF who provided information that may be incorporated in the RGI. Interested users are encouraged to access <http://glims.org/About/> for more information on GLIMS contributors, and http://nsidc.org/data/docs/noaa/g01130_glacier_inventory for more documentation on the WGI.

A detailed scientific description of the RGI, based on version 3.2, is given by Pfeffer et al. (2014).

2 Definitions of the RGI Regions

We define 19 first-order glacier regions drawn mostly from Radić and Hock (2010), with some minor modifications (Figure 1; Table 2). We further subdivide the first-order regions into second-order regions, of which there are 91 in total.

The region outlines have changed slightly between RGI versions, for example to avoid the splitting of glaciers between two regions or to make further analyses more convenient.

In RGI 6.0, the eastern boundaries of regions 13 (Central Asia) and 15 (South Asia East) were extended slightly to the east. A new second-order region 10-07 covering Japan was added to region 10 (North Asia). Region 08-01 (S Norway) was subdivided into regions 08-02 (SW Scandinavia) and 08-03 (SE Scandinavia), with former region 08-02 (N Scandinavia) assuming the code 08-01. Region 02-01 (Melville Island) was transferred to first-order region 03 (Arctic Canada North) as region 03-07, and the other second-order regions of region 02 (Western Canada and US) were renumbered as 02-01 to 02-05. These changes ensure the compatibility of the Glacier Regions dataset of the Global Terrestrial Network for Glaciers (GTN-G; http://www.gtn-g.ch/data_catalogue_glacreg/) with the RGI regions.

In RGI 5.0, the boundary between regions 01 (Alaska) and 02 (Western Canada and US) was refined, and in region 10 (North Asia) the former four second-order regions became six regions conforming with those described by Earl and Gardner (2016). In RGI 4.0, region 10-01, North Asia (North), was extended slightly to the west for better visibility of glaciers in the Polar Urals. Region 11-02, formerly the Pyrenees and Apennines, was enlarged and renamed Southern and Eastern Europe. First-order regions 10 (North Asia) and 11 (Central Europe) were enlarged accordingly.

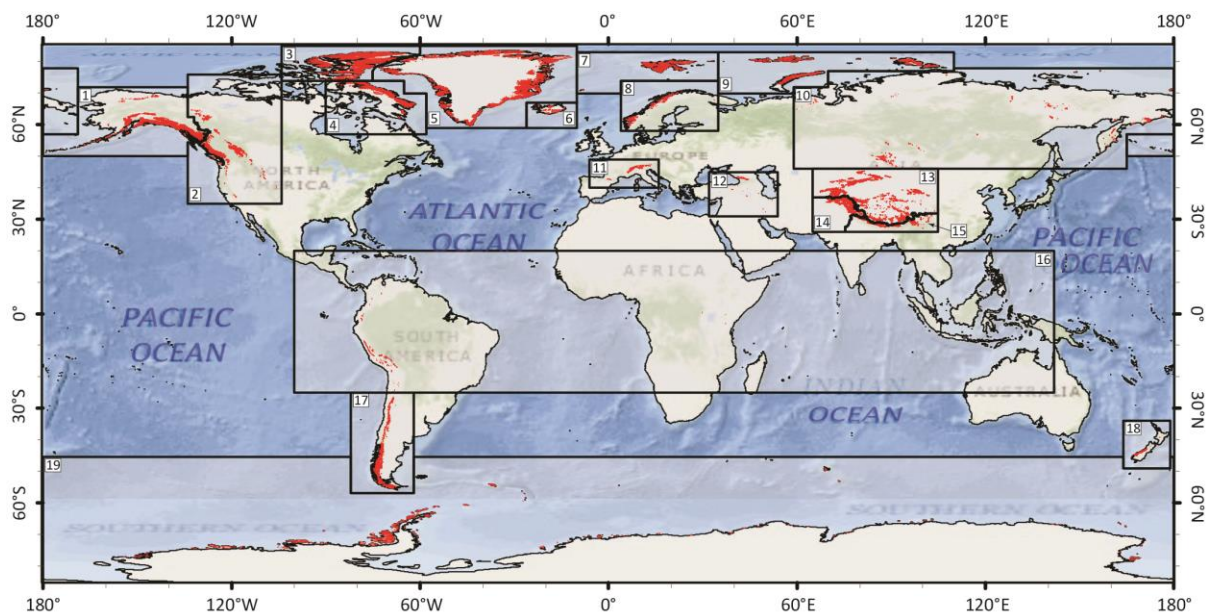


Figure 1. First-order regions of the Randolph Glacier Inventory (version 4.0).

First-order regions 01, 10 and 19 straddle the 180th meridian, and so do second-order regions 01-03 and 19-15. For convenience of analysis in a cylindrical-equirectangular coordinate system centred on

longitude 0°, as in Figure 1, each of these regions appears in the accompanying shapefiles as two polygons, eastern and western.

Table 2 – First- and second-order regions of the Randolph Glacier Inventory, version 6.0.

<i>First-order region</i>		<i>Second-order region (code, glacierized area in km², name)</i>		
01	Alaska	01-01	346	N Alaska
		01-02	16278	Alaska Ra (Wrangell/Kilbuck)
		01-03	1912	Alaska Pena (Aleutians)
		01-04	12052	W Chugach Mtns (Talkeetna)
		01-05	33174	St Elias Mtns
		01-06	22963	N Coast Ranges
02	Western Canada and USA	02-01	657	Mackenzie and Selwyn Mtns
		02-02	8803	S Coast Ranges
		02-03	4386	N Rocky Mtns
		02-04	529	Cascade Ra and Sa Nevada
		02-05	149	S Rocky Mtns
03	Arctic Canada (North)	03-01	27213	N Ellesmere Island
		03-02	11907	Axel Heiberg and Meighen Is
		03-03	21401	NC Ellesmere Island
		03-04	19294	SC Ellesmere Island
		03-05	10061	S Ellesmere Island (NW Devon)
		03-06	15124	Devon Island
		03-07	128	Melville Island
04	Arctic Canada (South)	04-01	4874	Bylot Island
		04-02	3324	W Baffin Island
		04-03	496	N Baffin Island
		04-04	8221	NE Baffin Island
		04-05	9919	EC Baffin Island
		04-06	7944	SE Baffin Island
		04-07	5843	Cumberland Sound
		04-08	247	Frobisher Bay
		04-09	20	Labrador
05	Greenland	05-01	89717	Greenland periphery
		05-11	—	Greenland Ice Sheet
06	Iceland	06-01	11060	Iceland
07	Svalbard and Jan Mayen	07-01	33837	Svalbard
		07-02	121	Jan Mayen
08	Scandinavia	08-01	1431	N Scandinavia
		08-02	1217	SW Scandinavia
		08-03	301	SE Scandinavia
09	Russian Arctic	09-01	12762	Franz Josef Land
		09-02	22128	Novaya Zemlya
		09-03	16701	Severnaya Zemlya
10	North Asia	10-01	15	Ural Mountains
		10-02	148	Central Siberia
		10-03	205	Cherskiy and Suntar Khayata Ranges
		10-04	1163	Altay and Sayan

		10-05	875	NE Russia
		10-06	4	E Chukotka
		10-07	0	Japan
11	Central Europe	11-01	2072	Alps
		11-02	3	Southern and Eastern Europe
12	Caucasus and Middle East	12-01	1256	Greater Caucasus
		12-02	51	Middle East
13	Central Asia	13-01	1846	Hissar Alay
		13-02	10234	Pamir (Safed Khirs/W Tarim)
		13-03	9531	W Tien Shan
		13-04	2854	E Tien Shan (Dzhungaria)
		13-05	8153	W Kun Lun
		13-06	3251	E Kun Lun (Altyn Tagh)
		13-07	1637	Qilian Shan
		13-08	7923	Inner Tibet
		13-09	3873	S and E Tibet
14	South Asia (West)	14-01	2938	Hindu Kush
		14-02	22862	Karakoram
		14-03	7768	W Himalaya
15	South Asia (East)	15-01	5447	C Himalaya
		15-02	4904	E Himalaya
		15-03	4383	Hengduan Shan
16	Low Latitudes	16-01	2338	Low-latitude Andes
		16-02	2	Mexico
		16-03	4	E Africa
		16-04	2	New Guinea
17	Southern Andes	17-01	25357	Patagonia
		17-02	3976	C Andes
18	New Zealand	18-01	1162	New Zealand
19	Antarctic and Subantarctic ^a	19-01	151	Subantarctic (Pacific)
		19-02	3751	South Shetlands and South Orkneys
		19-03	2523	Subantarctic (Atlantic)
		19-04	954	Subantarctic (Indian)
		19-05	662	Balleny Islands
		19-11	2714	E Queen Maud Land 7A
		19-12	554	Amery Ice Shelf 7B
		19-13	2765	Wilkes Land 7C
		19-14	590	Victoria Land 7D
		19-15	2590	Ross Ice Shelf 7E
		19-16	16916	Marie Byrd Land 7F
		19-17	403	Pine Island Bay 7G
		19-18	14861	Bellingshausen Sea 7H1
		19-19	61169	Alexander Island 7H2
		19-20	9288	W Antarctic Pena 7I1
		19-21	6385	NE Antarctic Pena 7I2
		19-22	770	SE Antarctic Pena 7I3
		19-23	0	Ronne-Filchner Ice Shelf 7J
		19-24	5821	W Queen Maud Land 7K

		19-31	—	Antarctic mainland
--	--	-------	---	--------------------

- a: In region 19 (Antarctic and Subantarctic) some second-order regions are named after their sector of the mainland; there are no mainland outlines in the RGI.

3 Data Description

3.1 Technical Specifications

The RGI is provided as shapefiles containing the outlines of glaciers in geographic coordinates (longitude and latitude, in degrees) which are referenced to the WGS84 datum. Data are organized by first-order region. For each region there is one shapefile (.SHP with accompanying .DBF, .PRJ and .SHX files) containing all glaciers and one ancillary .CSV file containing all hypsometric data. The attribute (.DBF) and hypsometric files contain one record per glacier.

Each object in the RGI conforms to the data-model conventions of ESRI ArcGIS shapefiles. That is, each object consists of an outline encompassing the glacier, followed immediately by outlines representing all of its nunataks (ice-free areas enclosed by the glacier). In each object successive vertices are ordered such that glacier ice is on the right. This data model is not the same as the current GLIMS data model, in which nunataks are independent objects.

The outlines of the RGI regions are provided as two shapefiles, one for first-order and one for second-order regions. A summary file containing glacier counts, glacierized area and a hypsometric list for each first-order and each second-order region is also provided. The 0.5°×0.5° grid is provided as a plain-text .DAT file in which zonal records of blank-separated glacierized areas in km² are ordered from north to south. Information about RGI glaciers that are present in the mass-balance tables of the WGMS database *Fluctuations of Glaciers* is provided as an ancillary .CSV file. The 19 regional attribute (.DBF) files are also provided in .CSV format.

3.2 Data Fields and Hypsometry

In version 5.0 the contents of the fields *RGIFlag* and *GlacType* were rearranged (see below). In version 4.0 six topographic attributes were added to the main shapefile entry for each glacier, with each glacier having a hypsometric list stored in a separate regional file. Each glacier had 12 data attributes in version 3.2 and 10 in version 2.0.

RGIId

A 14-character identifier of the form RGI vv - rr . $nnnnn$, where vv is the version number, rr is the first-order region number and $nnnnn$ is an arbitrary identifying code that is unique within the region. These codes were assigned as sequential positive integers at the first-order (not second-order) level, but they should not be assumed to be sequential numbers, or even to be numbers. In general the identifying code of each glacier, $nnnnn$, should not be expected to be the same in different RGI versions.

GLIMSIId

A unique 14-character identifier in the GLIMS format GxxxxxxEyyyyy Θ , where xxxxxx is longitude east of the Greenwich meridian in millidegrees, yyyyy is north or south latitude in millidegrees, and Θ is N or S depending on the hemisphere. The coordinates of *GLIMSIId* agree with *CenLon* and *CenLat* (see below).

Note that, even after the correction of former external *GLIMSIIds* described in the next paragraph, *GLIMSIIds* in the RGI are provisional. When RGI glaciers are incorporated into GLIMS, an existing GLIMS id code, if there is one, will replace the RGI code.

GLIMSIIds have been obtained in various ways, often visually, by different contributors to the RGI. In earlier versions, some were assigned by computing the centroid of the glacier polygon. In

consequence, some glaciers (fewer than 1%) had identifiers lying outside their boundaries. In version 4.0 all 1,560 of these exterior points were replaced by interior points. There were a further 324 replacements of interior points that were inside nunataks. The corresponding coordinates *CenLon* and *CenLat* (see below) were also altered. To identify interior points, the inward unit normals of all edges of the main glacier polygon were projected and clipped against the glacier polygon and any nunatak polygons. Among the midpoints of the resulting collection of line segments, that furthest from the glacier boundary was chosen for the *GLIMSId*.

RGIFlag

RGIFlag, together with *GlacType* (see below), was retired in version 6.0 in favour of a set of six separate attributes. The *RGIFlag|Snowcover* and *RGIFlag|Divides* flags, which had never been populated, were removed entirely. The former *RGIFlag|Status* is described below under *Status* and the former *RGIFlag|Connectivity* is described below under *Connect*.

BgnDate, EndDate

The date of the source from which the outline was taken, in the form *yyyymmdd*, with missing dates represented by -9999999. (The form for missing dates was -9990000 in RGI 3.0 and earlier.) When a single date is known, it is assigned to *BgnDate*. If only a year is given, *mmdd* is set to 9999. Only when the source provides a range of dates is *EndDate* not missing, and in this case the two codes together give the date range. In version 6.0, 98% of glaciers (by area; 99% by number) have date information (Figure 2). Figure 3 shows date-range spans for glaciers with date ranges. 85% of the ranges are shorter than four years. Many of the ranges of three years (36-47 months) are from the 1999–2003 period between the launch of Landsat 7 and the failure of the scan-line corrector of its ETM+ sensor.

CenLon, CenLat

Longitude and latitude, in degrees, of a single point representing the location of the glacier. These coordinates agree with those in *GLIMSId*.

O1Region, O2Region

The codes of the first-order and second-order regions (Table 2) to which the glacier belongs.

Area

Area of the glacier in km², calculated in cartesian coordinates on a cylindrical equal-area projection of the authalic sphere of the WGS84 ellipsoid, or, for nominal glaciers, accepted from the source inventory.

Zmin, Zmax

Minimum and maximum elevation (m above sea level) of the glacier, obtained in most cases directly from a DEM covering the glacier. For most of the nominal glaciers *Zmin* and *Zmax* were taken from the parent inventory, WGI or WGI-XF.

Zmed

Median elevation (m) of the glacier, chosen by sorting the elevations of the DEM cells covering the glacier and recording the 50th percentile of their cumulative frequency distribution.

The mean elevation of the glacier is not provided explicitly in the RGI but can be recovered with fair accuracy from the hypsometric list.

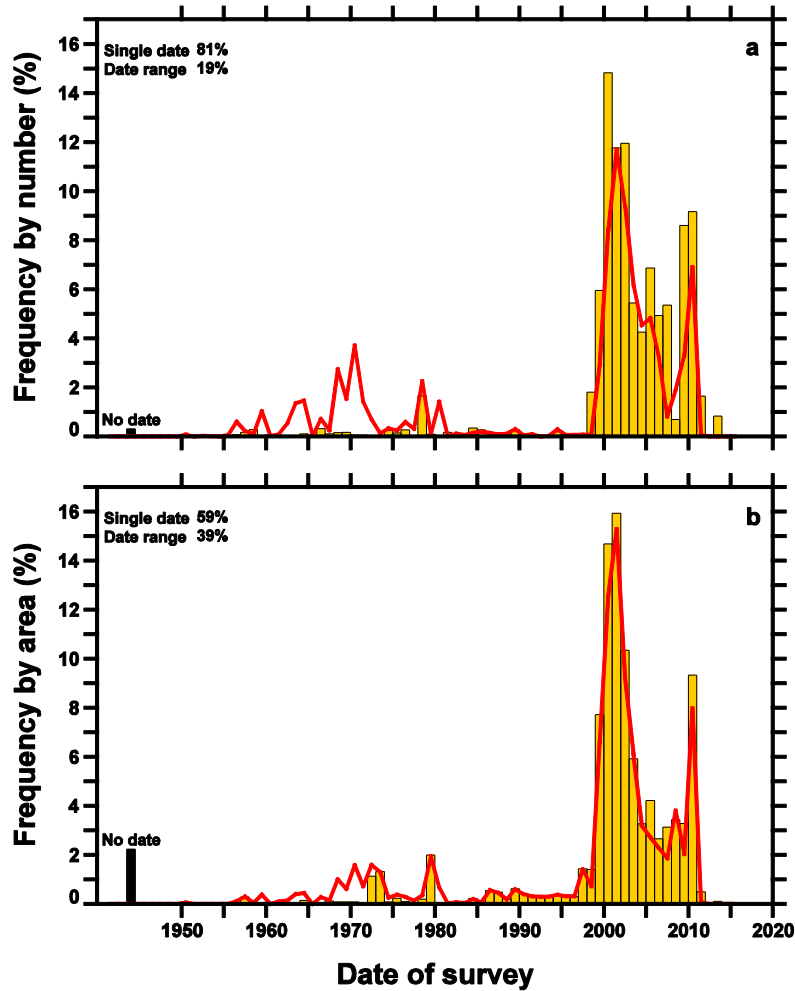


Figure 2. Distribution of dates in the RGI. Line: RGI 4.0; Bars: RGI 6.0. Glaciers with date ranges are assigned with uniform probability to each year of the range. The 633 undated glaciers are confined to regions 10 (Wrangell Island, North Asia), 11 (Italy, Central and Southern Europe) and 19 (Antarctic and Subantarctic).

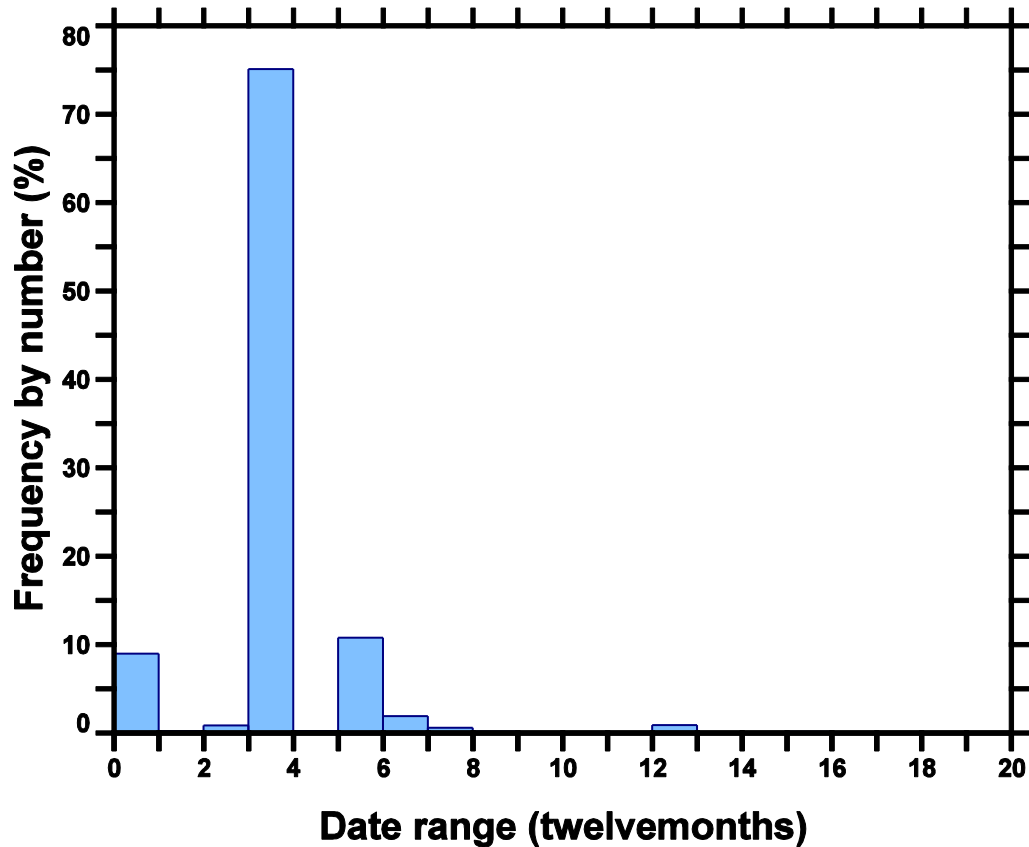


Figure 3. Frequency distribution of date ranges in the RGI. The ranges are numbers of months between *BgnDate* and *EndDate*, divided by 12.

Slope

Mean slope of the glacier surface (deg), obtained by averaging single-cell slopes from the DEM.

Aspect

The aspect (orientation) of the glacier surface (deg) is presented as an integer azimuth relative to 0° at due north. The aspect sines and cosines of each of the glacier’s DEM grid cells are summed and the mean aspect is calculated as the arctangent of the quotient of the two sums.

Lmax

Length (m) of the longest surface flowline of the glacier. The length is measured with the algorithm of Machguth and Huss (2014). Briefly, points on the glacier outline at elevations above *Zmed* are selected as candidate starting points and the flowline emerging from each candidate is propagated by choosing successive DEM cells according to an objectively weighted blend of the criteria of steepest descent and greatest distance from the glacier margin. The latter criterion can be understood as favouring “centrality”, especially on glacier tongues. The longest of the resulting lines is chosen as the glacier’s centreline. In Alaska, *Lmax* was calculated, only for glaciers larger than 0.1 km², as in Kienholz et al. (2014).

GlacType

GlacType, together with *RGIFlag* (see above), was retired in version 6.0 in favour of a set of six separate attributes. The flags formerly in *GlacType*, which were derived in part from Paul *et al.* (2009), are described below under *Form*, *TermType*, *Surging* and *Linkages*.

Status

The *Status* attribute flags glaciers whose outlines await subdivision or are nominal circles:

<i>Value</i>	<i>Status</i>
0	Glacier or ice cap
1	Glacier complex
2	Nominal glacier
9	Not assigned

Connect

The *Connect* attribute records the connectivity level developed by Rastner *et al.* (2012) for glaciers in Greenland. Glaciers that are physically detached from the ice sheet have a connectivity level of 0. A glacier is weakly connected if it is in contact with the ice sheet only at a well-defined divide in the accumulation zone, and strongly connected if the divide is indistinct in the accumulation zone and/or confluent with an ice-sheet outlet in the ablation zone:

<i>Value</i>	<i>Connect</i>
0	No connection
1	Weak connection
2	Strong connection
9	Not assigned

More details are given under Region 5: Greenland Periphery below.

Form

The *Form* attribute contains information on the form of the ice body:

<i>Value</i>	<i>Form</i>
0	Glacier
1	Ice cap
2	Perennial snowfield
3	Seasonal snowfield
9	Not assigned

TermType

The *TermType* attribute contains information on terminus type. Lake-terminating glaciers are identified as such only in Alaska, the Southern Andes and Antarctica; elsewhere they currently have *TermType* equal to 0. Where more than one value applies to a given terminus, the dominant type as interpreted from satellite imagery is chosen.

<i>Value</i>	<i>TerminusType</i>
0	Land-terminating
1	Marine-terminating
2	Lake-terminating
3	Dry calving
4	Regenerated
5	Shelf-terminating
9	Not assigned

Surging

The *Surging* attribute contains information on evidence for surging, and is based on the inventory of Sevestre and Benn (2015).

<i>Value</i>	<i>Surging</i>
0	No evidence
1	Possible
2	Probable
3	Observed
9	Not assigned

Linkages

The *Linkages* attribute indicates whether the ancillary file 00_RGI60_LINKS.CSV contains a link to mass-balance measurements in the *Fluctuations of Glaciers* database. To date 232 linkages have been identified.

<i>Value</i>	<i>Linkages</i>
0	Not in <i>FG</i>
1	In <i>FG</i>
9	Not assigned

Name

Name of the glacier, or the WGI or WGI-XF id code (modified after Müller et al., 1978) if available. Many glaciers do not have names, and coverage of those that do is incomplete. Of the 215,547 glaciers in RGI 6.0, 46,770 have information in their *Name* field, although for many the content is actually an id code. (The number of glaciers is 216,502 if Greenland glaciers strongly connected to the ice sheet are included.)

Hypsometry

The hypsometry list for each glacier, preceded by copies of the glacier's *RGIid*, *GLIMSId* and *Area*, is a comma-separated series of elevation-band areas in the form of integer thousandths of the glacier's total area (*Area*). The sum of the elevation-band areas is constrained to be 1000. This means that an elevation band's value divided by 10 represents the elevation band's area as a percentage of total glacier area. The elevation bands are all 50 m in height and their central elevations are listed in the file header record. Within each hypsometry file the elevation bands extend from 0–50 m up to the highest glacierized elevation band of the first-order region.

The hypsometry for Alaska was provided by C. Kienholz (Kienholz et al., 2014), relying on the Shuttle Radar Topography Mission DEM (SRTM) south of 60°N. North of 60°N, the elevation sources were a regional interferometric synthetic aperture radar DEM, a DEM from stereographic SPOT satellite imagery, and the ASTER GDEM2. The hypsometry for the Antarctic and Subantarctic is from Bliss et al. (2013). The primary DEM source was the DEM of the Radarsat Antarctic Mapping Project, with reliance also on the SRTM DEM and ASTER GDEM2, and on maps for some of the Subantarctic islands. Elsewhere the hypsometry was provided by M. Huss, relying on the SRTM DEM between 55°S and 60°N and, in version 5.0 and earlier, the ASTER GDEM2 and Greenland Mapping Project (GIMP) DEM north of 60°N (Huss and Farinotti, 2012). In version 6.0, some of the high-latitude hypsometry derived from the ASTER GDEM2, which as an optical sensor has difficulty over regions of featureless snow, was replaced with data from Viewfinder Panoramas (DEM3; <http://www.viewfinderpanoramas.org/>). The regions with hypsometry from this source are: Arctic Canada North (03), Arctic Canada South (04), Iceland (06), Svalbard(07), Scandinavia (08), Russian

Arctic (09) and parts of North Asia (10). It is intended that in a future version of the RGI the high-latitude hypsometry will be taken from the high-resolution ArcticDEM (Morin et al., 2017).

In version 6.0 as a whole, 1,466 glaciers (0.68%) have empty hypsometric lists (filled with the value -9; this value was 0 in version 4.0). Of these glaciers, 461 are nominal glaciers. The remaining omissions are attributable in some cases to technical shortcomings in the source DEMs, but more often to absence of any well-resolved DEM at all.

Linkages

The file 00_RGI60_LINKS.CSV provides basic information (*RGIId*, *GLIMSId*, *Name*, *Area*, *CenLon*, *CenLat*) for each RGI glacier with *Linkages* equal to 1, as well as the primary key *FoGId* of the glacier in the WGMS *Fluctuations of Glaciers* database and information about its mass-balance record therein. Most of the linkage information was provided by V. Radić, R. Lo, F. Maussion and J. Landmann.

3.3 Glacier Delineation

Glacier outlines that were separated from their neighbours when received were accepted without change, subject only to the quality control described below. However many glacier outlines were originally obtained or contributed as glacier complexes, that is, as collections of contiguous glaciers that meet at glacier divides. We used semi-automated algorithms (Bolch et al., 2010a; Kienholz et al., 2013) to separate these complexes into glaciers. The quality of raw output from the algorithms primarily depends on the quality of the digital elevation model (DEM) available for a particular region. Even when a high-quality DEM is available the algorithm output requires some manual checking. These checks were carried out in detail only in Alaska, Western Canada and US, Arctic Canada South, Greenland and parts of the Asian regions 13, 14 and 15. In the Alps, divides between glaciers were adopted from previous glacier inventories. Elsewhere, in many cases further work is necessary to inspect the quality of drainage divides.

3.4 Quality Control

Quality checks were conducted on all glacier polygons. These include geometry, topology and attribute-field checks. As of version 3.2, the following steps are carried out:

- 1) The ArcGIS Repair Geometry tool is run on all polygons. Among other tasks, this routine checks for polygon closure, corrects the ring ordering and eliminates duplicate vertices.
- 2) Glaciers with areas less than 0.01 km², the recommended minimum of the WGI, are removed. Nunataks are retained whatever their area.
- 3) A common error occurs when glacier polygons are adjusted during editing without ensuring that the shared boundary with an adjacent polygon is also updated (for example, at a glacier divide). Such errors result in overlapping polygons, or gaps between polygons, yielding small “sliver” polygons that must be removed or corrected. To check for these errors we constructed topology rules within ArcGIS. We began by checking topology using the ‘Does Not Overlap’ rule. Next, we removed each glacier with errors and wrote it to its own single-polygon shapefile. In an iterative procedure, each single glacier was updated on all others, such that areas with overlap were eliminated. The final subset of corrected outlines was merged back into the set of error-free outlines.
- 4) Attribute tables are checked, using Fortran subroutines and scripts written in Python, for things such as empty fields, GLIMSIds outside their glaciers, incorrectly formatted dates, incorrect assignments to RGI regions, and inconsistent minimum and maximum elevations.

4 Revisions in RGI 6.0

4.1 Overview

An overview is given here. Detailed information in the form of a revision log is provided by region in Chapter 5.

In most regions, glacier outlines are unchanged between RGI 5.0 and 6.0, but those in the conterminous US (regions 02-04 and 02-05) have been replaced entirely and those in Scandinavia (region 08) have been augmented substantially, while outlines now replace the previous nominal glaciers in Iran (region 12-02), France and Italy (region 11-01).

Surging codes were added based on the global inventory of Sevestre and Benn (2015). In total, 1343 RGI 6.0 glaciers have codes identifying them as possible (511), probable (384) or observed (448) surge-type glaciers. This total is less than that of Sevestre and Benn (2015), who were able in many cases to assign codes to distinct tributary glaciers. The No-evidence code (*Surging* = 0) was assigned to 42,515 glaciers that have been assessed in systematic regional searches for evidence of surging (e.g. Björnsson et al. 2003; Clarke et al., 1986; Copland et al. 2003, 2011; Osipova et al., 1998). The remaining 172,644 glaciers have yet to be assessed individually and have the Unassigned code (*Surging* = 9).

4.2 Known Flaws

Nominal glaciers remain in regions 8 (Scandinavia: Kola Peninsula, 4 glaciers, 1 km²), 10 (North Asia: De Long Islands, Wrangell Island; 116 glaciers, 84 km²), 2 (Central Europe: Slovenia 0.03 km²), and 12 (Caucasus and Middle East: western and eastern Greater Caucasus, Lesser Caucasus; 339 glaciers, 156 km²).

In addition, outlines in a number of regions are known to have errors. For example, in South Georgia (region 19-03) and in the Southern Andes (region 17) some outlines are known or believed to include seasonal snow.

It is intended that future releases of the RGI will improve these and other shortcomings.

5 Description of Data Compilation by Region

5.1 REGION 1: Alaska

Contributor	Institution	Project/Funding
Arendt, A. Herreid, S. Hock, R. Kienholz, C. Rich, J.	University of Alaska Fairbanks, USA	National Park Service, Geophysical Institute, NASA Cryospheric Sciences, National Science Foundation (US), Geographic Information Network of Alaska
Beedle, M.	University of Northern British Columbia, Canada	
Berthier, E.	CNRS-OMP-LEGOS, France	French Space Agency (CNES)
LeBris, R. Frey, H. Paul, F. Bolch, T.	University of Zürich, Switzerland	GlobGlacier/ESA
Burgess, E. Forester, R. Lund, J.	University of Utah, USA	
Giffen, B.	National Park Service, USA	
Hall, D.	NASA Goddard Space Flight Center, USA	
Manley, W.	INSTAAR, USA	

The Alaska region encompasses all glaciers in the state of Alaska, USA, and also all those glaciers in the Yukon Territory and British Columbia, Canada, that are part of the icefields that straddle the US/Canada border. On its southeastern boundary, the region ends just north of Prince Rupert, British Columbia and just south of the end of the Alaska border. From there the region extends inland to the divide between Gulf of Alaska and Arctic drainages.

Changes from Version 5.0 to 6.0

None.

Changes from Version 4.0 to 5.0

The boundary between region 01-06 (N Coast Ranges) and regions 02-03 (S Coast Ranges) and 02-04 (N Rocky Mtns) was refined, with transfers of three glaciers to region 01-06 from 02-03 and four to 02-03 from 01-06 in consequence.

Links were added to 7 glaciers in the WGMS mass-balance database.

Changes from Version 3.2 to 4.0

A new inventory (Kienholz et al., 2015), including topographic and hypsometric attributes, replaces the former inventory of Alaska.

We checked and, if necessary, adapted glacier divides using measured velocity fields from Burgess and others (2013), resulting in substantial changes in many glacier outlines. The velocity fields cover all major icefields and roughly 50% of the total Alaskan glacierized area. Differences are most substantial for icefields and for glaciers with divides initially derived from the USGS DEM from the 1950s (e.g., Harding Icefield, Figure 4) rather than more modern DEMs. We also checked for remaining outlining errors (e.g., snow misclassified as ice) and adapted outlines manually where necessary. The updated outlines were used to derive the topographic and hypsometric attributes from the modern DEMs (Kienholz et al., 2014). In addition, we completed the RGI fields *GlacType* and *BgnDate* for all glaciers and added more glacier names, such that 585 glaciers now have names allocated.

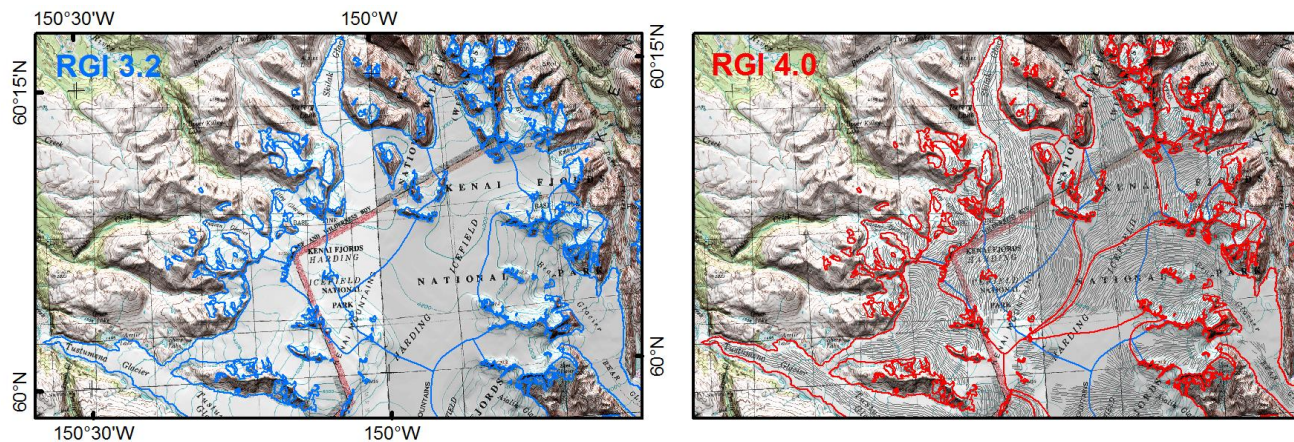


Figure 4. Harding Icefield. Glacier divides derived from the USGS 1950 maps (left) and modern-date divides including velocity fields (right side) superimposed on the 1950 USGS base map.

Changes from Version 3.0 to 3.2

None.

Changes from Version 2.0 to 3.0

Additional improvements were made to the St. Elias, Lake Clark and Juneau Icefields regions. All remaining DCW outlines were replaced with more detailed recent outlines.

Changes from Version 1.0 to Version 2.0

Three glaciers in the Kigluaik Mountains of western central Alaska (01-01) were added as nominal circles from WGI-XF.

Glaciers in Katmai and Lake Clark National Parks have been updated to 2006-2010 IKONOS imagery.

The entire Stikine Icefield region has been updated using modern imagery.

Glaciers at the head of Lynn Canal, and in the eastern portion of the Western Chugach Mountains near Cordova, have been updated.

Extensive improvements have been made to the Wrangell/St. Elias region. What is included in RGI version 2.0 is a partially edited version of Berthier et al.'s (2010) and Beedle et al.'s (2008) outlines, updated to circa 2010 Landsat 7 ETM+ imagery for the Wrangell Mountains, 2006-2010 IKONOS imagery for the US portion of St. Elias, and Canadian topographic maps for the Canadian portion of the St. Elias. Between V1.0 and V2.0 we have focused on capturing the largest area changes occurring primarily at low elevations; however some regions remain unmodified between V1.0 and V2.0.

Version 1.0

Numerous groups contributed Alaska glacier outlines. Le Bris et al. (2011) mapped the Kenai Peninsula, Tordillo, Chigmit and Chugach Mountains using Landsat TM scenes acquired between 2005-2009. They used automated (band-ratioing) glacier mapping techniques with additional manual editing to deal with incorrect classification of debris-covered glaciers. Drainage divides in the accumulation region were derived from the USGS DEM. Bolch et al. (2010) contributed outlines for the Coast Mountains.

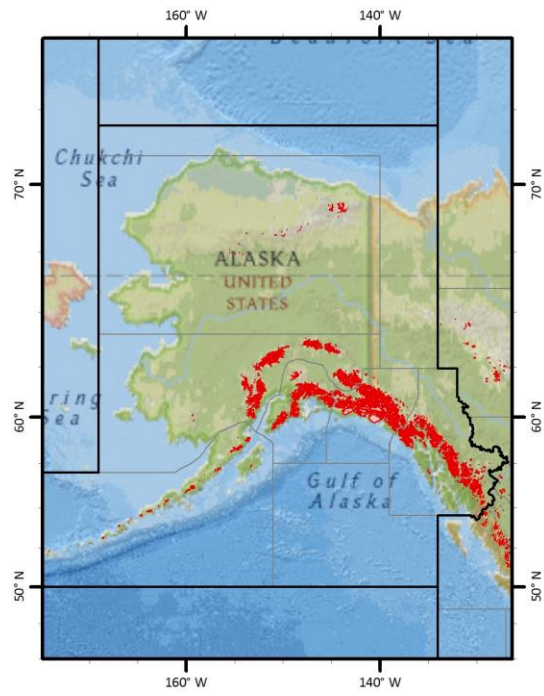
As part of a mapping effort by the National Park Service (NPS), the University of Alaska Fairbanks (UAF) has been mapping all glaciers in NPS boundaries, as well as glaciers connected to but not within park boundaries, for two time periods (USGS 1950s map dates, and most recent satellite imagery). For this effort UAF has in many regions started with existing, older outlines and updated them to the most modern imagery available. These include outlines from Berthier et al. (2010), Beedle et al. (2008), and outlines provided by B. Giffen, D.K. Hall and W.F. Manley. UAF has updated these outlines to circa 2010 pan-sharpened 15 m resolution Landsat 7 ETM+ scenes, 5 m resolution imagery from the SPOT SPIRIT initiative (dating approximately 2007; Korona et al., 2009) and 2006-2010 IKONOS imagery. UAF Geophysical Institute internal funding and National Science Foundation funding has also been used to support digitizing efforts in the Alaska Range, Chugach Mountains and Juneau Icefield glaciers. Nearly all of these regions are based on 2010 imagery.

The University of Utah (E.W. Burgess, R.R. Forester, J. Lund) created outlines for the Stikine Icefield region derived from 1980s Landsat 5 imagery.

W.F. Manley provided all outlines for Brooks Range glaciers.

Glaciers along the Aleutian Island chain are taken from Berthier et al. (2010).

Glaciers other than those mapped by Le Bris et al. (2011) were delineated using an automated algorithm described by Kienholz et al. (2013). USGS digital elevation models as well as the ASTER GDEM v1 were used as sources of elevation information.



5.2 REGION 2: Western Canada and US

Contributor	Institution	Project/Funding
Bolch, T.* Menounos, B. Wheate, R.	University of Northern British Columbia, Canada * Now at University of Zürich, Zürich, Switzerland	WC2N/CFCAS
Fountain, A.G. Hoffman, M.J.	Portland State University, USA Los Alamos National Laboratory, USA	

Changes from Version 5.0 to 6.0

The seven glaciers on Melville Island were transferred from former region 02-01 to region 03-07, with ids 03.04552 to 03.04558.

In regions 02-04 (Cascade Ra and Sa Nevada) and 02-05 (S Rocky Mtns), all but a few Canadian outlines were replaced from an inventory taken from maps of scale 1:24,000 (Fountain et al., 2007) and from outlines provided for Rocky Mountain National Park by M. Hoffman (Hoffman et al., 2007). (These regions were formerly numbered 02-05 and 02-06.) The previous coverage, also from Fountain et al. (2007), was from 1:100,000-scale maps. In consequence the glacier counts in the two regions increased several-fold, to 3202 in region 02-04 and 1967 in region 02-05, and their total areas increased to 529 km² and 149 km² respectively. The new outlines all have dates, unlike the old outlines, and it was possible to identify all 28 of those with measurements in the WGMS mass-balance database. The map dates range from the 1940s to the 1980s. The Rocky Mountain National Park outlines are from 2001.

Changes from Version 4.0 to 5.0

The boundary between region 01-06 (N Coast Ranges) and regions 02-03 (S Coast Ranges) and 02-04 (N Rocky Mtns) was refined, with transfers of three glaciers to region 01-06 from 02-03 and four to 02-03 from 01-06 in consequence.

Links were added to 21 glaciers in the WGMS mass-balance database.

Changes from Version 3.2 to Version 4.0

145 exterior *GLIMS*Ids were replaced. Topographic and hypsometric attributes (section 3.2) were added.

Changes from Version 3.0 to 3.2

None.

Changes from Version 2.0 to Version 3.0

Glacier complexes were separated into single glaciers in the northern part of the region.

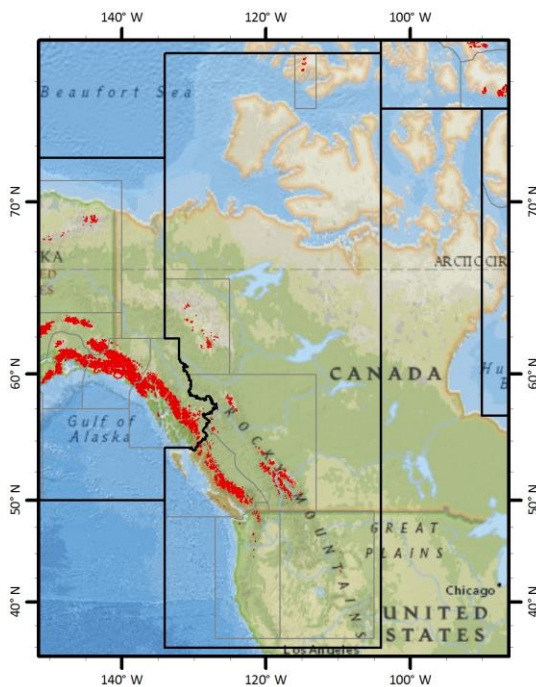
Changes from Version 1.0 to Version 2.0

The glaciers on Melville Island (region 02.01) were represented in version 1.0 by DCW outlines and have been replaced by Canvec outlines taken from Region 03. DCW outlines for the Mackenzie Mountains and Selwyn Mountains (region 02-02), on the boundary between Yukon and the North West Territories, were replaced by Canvec outlines provided by M. Sharp and J.G. Cogley.

Version 1.0

Glaciers in BC and Alberta were mapped using orthorectified Landsat 5 TM scenes from the years 2004 and 2006 obtained by British Columbia Government, Ministry of Forests and Range. We selected the TM3/TM5 band ratio for glacier mapping. For the entire study area, we used improved British Columbia TRIM glacier outlines as a mask to minimize misclassification due to factors such as seasonal snow. When using this mask, we assumed that glaciers did not advance between 1985 and 2005, an assumption that holds for practically all non-tidewater glaciers in western North America. The mask also maintained consistency in the location of the upper glacier boundary and the margins of nunataks. This consistency is important where seasonal snow hampers correct identification of the upper glacier boundary. We mapped only glaciers larger than 0.05 km², as a smaller threshold would include many features that were most likely snow patches. In addition, all snow and ice patches that were not considered to be perennial ice in the TRIM data were eliminated and hence, we minimize deviations in glacier areas that could arise from interpretative errors or major variations in snow cover. The resulting glacier polygons were visually checked for gross errors based on the procedures previously discussed, and fewer than 5% of the glaciers were manually improved. We derived glacier drainage basins based on a flowshed algorithm using the TRIM DEM and a buffer around each glacier. More information can be found in Bolch et al. (2010a).

Data for the US south of 49°N (Fountain et al., 2007; <http://glaciers.us>) were derived from the GLIMS database.



5.3 REGION 3: Arctic Canada North

Contributor	Institution	Project/Funding
Gardner, A.	Clark University, Worcester, USA (now at Jet Propulsion Laboratory, California Institute of Technology, USA)	
Wolken, G.	Department of Geological and Geophysical Surveys, Alaska, USA	
Barrand, N. Cawkwell, F. Copland, L. Filbert, K. Hartmann, G. O'Callaghan, P. Sharp, M. Wyatt, F.	University of Alberta, Canada	
Burgess, D.	Natural Resources Canada	
Paul, F.	University of Zürich, Switzerland	GlobGlacier/ESA

Changes from Version 5.0 to 6.0

Glacier complex RGI50-03.04540, added in version 5.0, was subdivided into 11 outlet glaciers with ids 03.04541 to 03.04551. The seven glaciers on Melville Island were transferred from former region 02-01 to region 03-07, with ids 03.04552 to 03.04558.

The source for hypsometry was changed from the ASTER GDEM2 to the ViewfinderPanoramas DEM3 (<http://www.viewfinderpanoramas.org/>).

Changes from Version 4.0 to 5.0

Names were assigned to some glaciers on Axel Heiberg Island. Glacier RGI40-03.00840 was subdivided into RGI50-03.04538 (Thompson Glacier) and RGI50-03.04539 (White Glacier). Alexander Trishchenko (Canada Centre for Remote Sensing, Ottawa) pointed out that an ice cap of 126 km² on Colin Archer Peninsula, northwest Devon Island was missing, and it was added (RGI50-03.04540).

Links were added to 4 glaciers in the WGMS mass-balance database.

Changes from Version 3.2 to 4.0

One exterior *GLIMS*id was replaced. Topographic and hypsometric attributes (section 3.2) were added.

Changes from Version 3.0 to 3.2

Glaciers were delineated from the glacier complexes using the delineation algorithm developed by Kienholz et al. (2013) and applied to the 1:250000 Canadian Digital Elevation Data (CDED). Some minor manual editing was done to remove obvious blunders.

Changes from Version 2.0 to 3.0

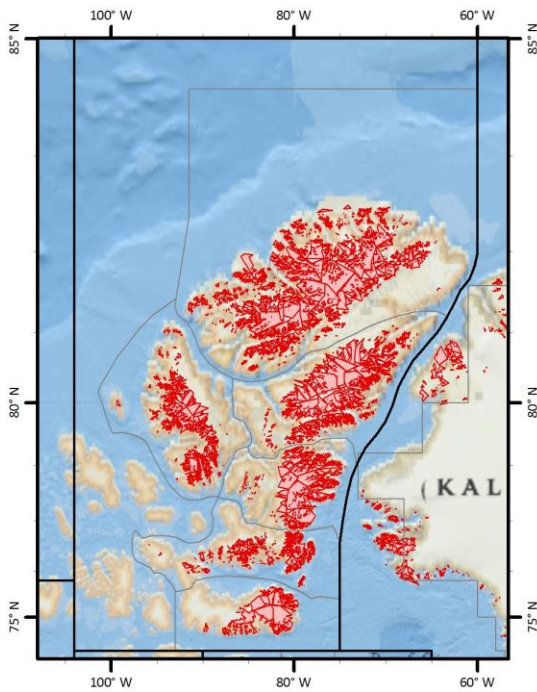
Changes from Version 1.0 to Version 2.0

Canvec outlines of the Melville Island glaciers, which were mistakenly duplicated in region 03 in version 1.0, were transferred to region 02.

Version 1.0

Glacier outlines were created from late summer, cloud-free 1999-2003 Landsat 7 (ETM+) imagery and from 2000-2003 ASTER imagery. A normalized-difference snow index (NDSI) was calculated for all Landsat imagery to identify snow- and ice-covered terrain. Empirically derived thresholds were applied to refine these classifications and to separate snow from glacier ice. A clumping procedure was then applied to the classified snow and ice data to delineate contiguous groups of pixels, followed by an elimination procedure, which removed small clusters of non-ice pixels. Gridded snow and ice data were then converted to polygons and edited manually to correct misclassifications. Small portions of some areas within this region were not adequately imaged by Landsat, due to either persistent cloudiness or shadowing. Consequently, in these areas manual digitization of ASTER imagery was used to capture glacier outlines.

Outlines for Devon Island were provided by D. Burgess and were derived from 1999/2000 velocity maps.



5.4 REGION 4: Arctic Canada South

Contributor	Institution	Project/Funding
Gardner, A.	Clark University, Worcester, USA (now at Jet Propulsion Laboratory, California Institute of Technology, USA)	
Wolken, G.	Department of Geological and Geophysical Surveys, Alaska, USA	
Barrand, N. Cawkwell, F. Copland, L. Filbert, K. Hartmann, G. O'Callaghan, P. Sharp, M. Wyatt, F.	University of Alberta, Canada	
Burgess, D.	Natural Resources Canada	
Paul, F.	University of Zürich, Switzerland	GlobGlacier/ESA

Changes from Version 5.0 to 6.0

Seven pairs of glacier outlines in east-central Baffin Island were found to have spurious divides that were actually the edges of maps. These pairs were merged: the surviving members of each pair, with the deleted members in parentheses, are RGI60-04.00408 (04.00465); 04.00413 (04.00415); 04.00416 (04.00412) 04.00420 (04.00419); 04.00424 (04.00425); 04.00433 (04.00423); 04.00467 (04.00464).

The source for hypsometry was changed from the ASTER GDEM2 to the ViewfinderPanoramas DEM3 (<http://www.viewfinderpanoramas.org/>).

Changes from Version 4.0 to 5.0

All glaciers in region 04-09, Labrador, were replaced with information from the inventory of Way et al. (2014).

Links were added to 5 glaciers in the WGMS mass-balance database.

Changes from Version 3.2 to 4.0

Eight exterior *GLIMS*IDs were replaced. Topographic and hypsometric attributes (section 3.2) were added.

Glacier 04.06811, which duplicated glacier 04.06813 in version 3.2, was removed.

Changes from Version 3.0 to 3.2

Glaciers were delineated from the glacier complexes using the delineation algorithm developed by Kienholz et al. (2013) and applied to the 1:250000 Canadian Digital Elevation Data (CDED). Some minor manual editing was done to remove obvious blunders.

Changes from Version 2.0 to 3.0

None.

Changes from Version 1.0 to Version 2.0

Outlines for 27 glaciers in Labrador (region 04-09) were added, provided by P. O'Callaghan, N. Barrand, F. Wyatt and M. Sharp, University of Alberta.

Version 1.0

Glacier complex outlines were compiled from 214 CanVec maps, a digital cartographic reference product of Natural Resources Canada. An additional 5500 km² of glacier area in central Baffin Island not covered by Edition 9 of the CanVec data set were taken from an expanded inventory based on Paul and Kääb (2005) and Svoboda and Paul (2009). All outlines in this expanded inventory were created from late-summer Landsat 7 ETM+ imagery acquired between 1999 and 2002. Of the CanVec maps, 13 were based on late-summer SPOT 5 imagery acquired between 2006–2010 and seven on 1958 or 1982 aerial photographs. A small fraction of ice coverage is missed by the Canvec dataset because of incorrect classification over debris-covered ice and supraglacial lakes. The misclassification is very noticeable for outlet glaciers where medial moraines are not identified as glacier ice. Glaciers were delineated with the algorithm of Kienholz et al. (2013) and edited manually where necessary.

5.5 REGION 5: Greenland Periphery

Contributor	Institution	Project/Funding
Rastner, P. Mölg, N. Bolch, T. LeBris, R. Paul, F.	University of Zürich, Switzerland	ice2sea/EU FP7 GlobGlacier/ESA Glaciers_cci/ESA
Howat, I. Negrete, A.	Byrd Polar Research Center, Ohio State University, USA	

Changes from Version 5.0 to 6.0

None.

Changes from Version 4.0 to 5.0

None.

A link was added to the record of Mittivakkat Glacier in the WGMS mass-balance database.

Changes from Version 3.2 to 4.0

46 exterior *GLIMS*IDs were replaced. Topographic and hypsometric attributes (section 3.2) were added.

19 glaciers appeared twice in version 3.2. One member of each such pair was removed.

Changes from Version 3.0 to 3.2

A planimetric offset was discovered in parts of Greenland in version 3.0. This offset was repaired.

Changes from Version 2.0 to Version 3.0

Coverage of Greenland is new in version 3.0, and is described in detail by Rastner et al. (2012). In all, 73 satellite images were processed. Glacier complexes were subdivided using a flowshed algorithm. An enhanced form of the algorithm for identifying glaciers other than the Greenland Ice Sheet was developed. In addition to the connectivity rule described below (see Version 1.0), a “topographic heritage rule” was added. Glaciers adjoining the ice sheet were first assigned to level CL2 (strongly connected) or level CL1 (weakly connected). Unassigned glaciers adjoining one or more level-2 glaciers were then assigned the same connectivity, and likewise for glaciers adjoining level-1 glaciers. The remaining unassigned glaciers, those not connected to the ice sheet at all, were assigned to level CL0. The result of these operations is summarized in Table3.

Table 3 – Number and extent of glaciers in Greenland

<i>Connectivity Level</i>	<i>Number</i>	<i>Area (km²)</i>
CL0	17 508	65 473
CL1	1 815	24 244
CL2	957	40 354
Ice sheet	1	1 678 497
Total	20 281	1 808 568

Glaciers of all three connectivity levels are included in the RGI. Rastner et al. recommend that CL2 glaciers be treated as part of the ice sheet, for which purpose they can be identified using *Connect*. The total extent of CL0 and CL1 glaciers, 89731 km², is well in excess of any previous estimate of the extent of glaciers in the Greenland periphery. Adding the CL2 glaciers and the ice sheet, Rastner et al. estimate a glacierized area for Greenland as a whole of $1.808 \pm 0.004 \times 10^6$ km². This lies between the two estimates suggested by Kargel et al. (2012), $1.801 \pm 0.016 \times 10^6$ km² and $1.824 \pm 0.016 \times 10^6$ km²; these estimates are statistically indistinguishable from but more uncertain than that of Rastner et al.

Changes from Version 1.0 to Version 2.0

None.

Version 1.0

Distinguishing between what is considered ice sheet versus glaciers is a challenge, and depends on the scientific application. While the distinction is clear for the numerous fully detached glaciers, there are several regions where, although there is a physical connection to the main ice sheet, the ice mass is either a valley glacier in mountainous terrain, or it forms its own ice dome and is largely uncoupled from the ice sheet dynamics. Therefore, for applications such as extrapolation of laser altimetry data, some researchers consider that such ice masses should be categorized as glaciers rather than as part of the ice sheet.

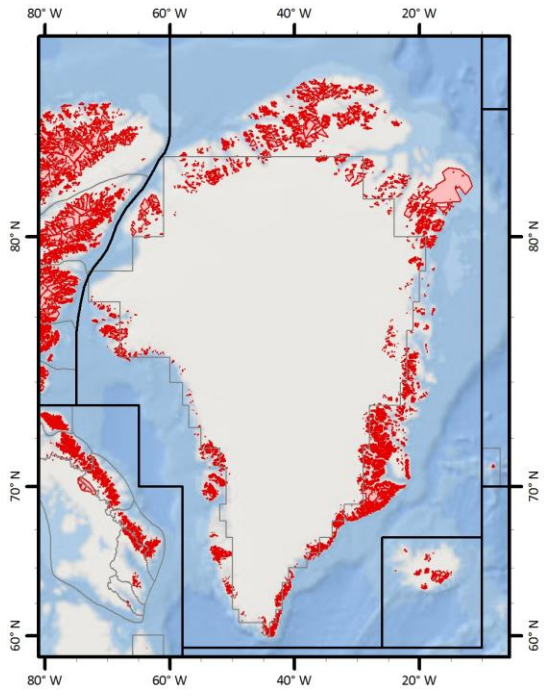
In the RGI, all ice masses with a possible but uncertain drainage divide are assigned to the ice sheet (e.g. on the Geikie Plateau), and all others to the local (or peripheral) glaciers. The latter are either:

- not connected to the ice sheet at all
- clearly separable (e.g. by mountain ridges) in the accumulation region, or
- only in contact with ice sheet outlets in the ablation region.

Indeed, there is room for discussion on individual decisions, but for the purpose of the RGI we just need to start somewhere. The separation in the accumulation area is done along drainage divides derived from DEM-based watershed analysis.

The glaciers north of $\sim 81^\circ\text{N}$ were not available from Landsat data and were provided by the Greenland Mapping Project (Howat et al., 2014).

The semi-automated glacier mapping applied to the 64 Landsat scenes that were processed is based on a band ratio (ETM+ Band 3/Band 5) with an additional threshold in band 1 for better mapping of glacier areas in cast shadow. It is based on Paul and Kääb (2005) and described for a part of western Greenland in Citterio et al. (2009). Debris-covered glacier parts as well as wrongly classified sea ice, icebergs or lakes were corrected manually in the vector domain. A 3 by 3 median filter is applied for image smoothing and glaciers smaller than 0.05 km² are not considered. Wrongly classified regions with seasonal snow could not always be corrected.



5.6 REGION 6: Iceland

Contributor	Institution	Project/Funding
Sigurðsson, O.	National Energy Authority, Iceland	

Changes from Version 5.0 to 6.0

The source for hypsometry was changed from the ASTER GDEM2 to the ViewfinderPanoramas DEM3 (<http://www.viewfinderpanoramas.org/>).

Changes from Version 4.0 to 5.0

None.

Links were added to 9 glaciers in the WGMS mass-balance database.

Changes from Version 3.2 to 4.0

One exterior *GLIMSid* was replaced. Topographic and hypsometric attributes (section 3.2) were added.

Changes from Version 2.0 to Version 3.2

Glaciers were delineated from the glacier complexes.

Changes from Version 2.0 to Version 3.0

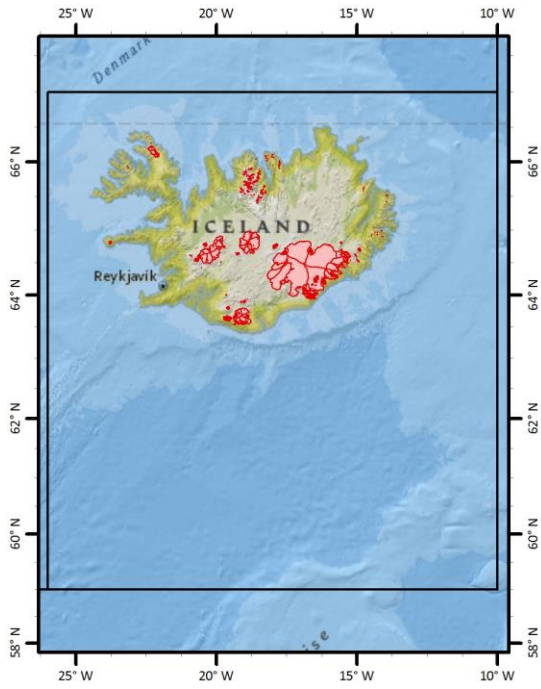
None.

Changes from Version 1.0 to Version 2.0

None.

Version 1.0

Outlines of glacier complexes in Iceland were added to the GLIMS database by O. Sigurðsson and extracted therefrom by J.G. Cogley, who merged nunataks with the glacier complexes containing them. Most outlines were acquired from 1999–2004 ASTER and SPOT5 imagery; some in the north of Iceland were acquired from oblique aerial photographs.



5.7 REGION 7: Svalbard

Contributor	Institution	Project/Funding
König, M., Kohler, J.	Norwegian Polar Institute, Norway	Cryoclim/ESA
Hagen, J-O., Nuth, C., Moholdt, G.	University of Oslo, Norway	Cryoclim and Glaciers_cci/ESA
Pettersson, R.	Uppsala University, Sweden	

Changes from Version 5.0 to 6.0

The source for hypsometry was changed from the ASTER GDEM2 to the ViewfinderPanoramas DEM3 (<http://www.viewfinderpanoramas.org/>).

Changes from Version 4.0 to 5.0

Links were added to 10 glaciers in the WGMS mass-balance database.

Changes from Version 3.2 to Version 4.0

One exterior *GLIMS*id was replaced. Topographic and hypsometric attributes (section 3.2) were added.

In earlier versions, dates were omitted for 119 glaciers (total area 9,770 km²). They have now been restored from the inventory of Nuth et al. (2013). The new dates were extracted from file CRYOCLIM_GAO_SJ_2001-2010.ZIP, downloaded from <https://data.npolar.no/dataset/89f430f8-862f-11e2-8036-00505bad0004>. The newly-dated glaciers, RGI40-07.01449 to RGI40-07.01567, were matched on-screen one by one between RGI 4.0 and the Nuth shapefile.

Changes from Version 3.0 to 3.2

None.

Changes from Version 2.0 to 3.0

None.

Changes from Version 1.0 to Version 2.0

Outlines of the glaciers on Jan Mayen (07-02) were digitized by J.G. Cogley from Hagen et al. (1993).

Version 1.0

The Svalbard inventory is described in more detail by Nuth et al. (2013).

Three primary data sets are used. The main sources are SPOT5-HRS DEMs and orthoimages provided within the framework of the IPY-SPIRIT (SPOT 5 stereoscopic survey of Polar Ice: Reference Images and Topographies) Project (Korona et al., 2009). The SPOT5-HRS collects 5m panchromatic stereo images that are stereoscopically processed into 40m DEMs, then used to generate the orthoimages. Five SPIRIT scene acquisitions from 2007-2008 cover 71% of the glacier area. The secondary source is 23 scenes from the ASTER sensor in the form of automatically generated DEMs and orthoimages (AST14DMO products downloaded from NASA) covering 16% of the glacier area. Cloud-free scenes are not available for 2007-2008, and therefore data from as early

as 2001 are used. For less than 14% of the glacier area, a suitable SPOT5-HRS or ASTER scene was not available. For these glaciers, 11 orthorectified Landsat scenes are used. Furthermore, additional Landsat and ASTER scenes are used to aid digitization decisions about the seasonal snow cover.

The original glacier delineation and glacier identification system is based on the Hagen et al. (1993) atlas, which conforms to WGI standards but is only available as a hard copy. Therefore, digitized national datasets are the base glacier masks from which to begin the inventory (König et al, 2013). From this original dataset, we manually re-delineated the individual glacier basins based upon the Hagen et al. (1993) *Atlas* and updated by trimming the front position and the lateral edges below the ELA. Since the original national dataset was derived by cartographers, many of the mask segments above the ELA contained snow covered valley walls and gullies (not perennially snow covered). These are, to the best of our ability, clipped from the masks by visually analyzing the recent satellite archives of ASTER and Landsat. Figure 5 summarizes the distribution of imagery dates used to generate the Svalbard outlines.

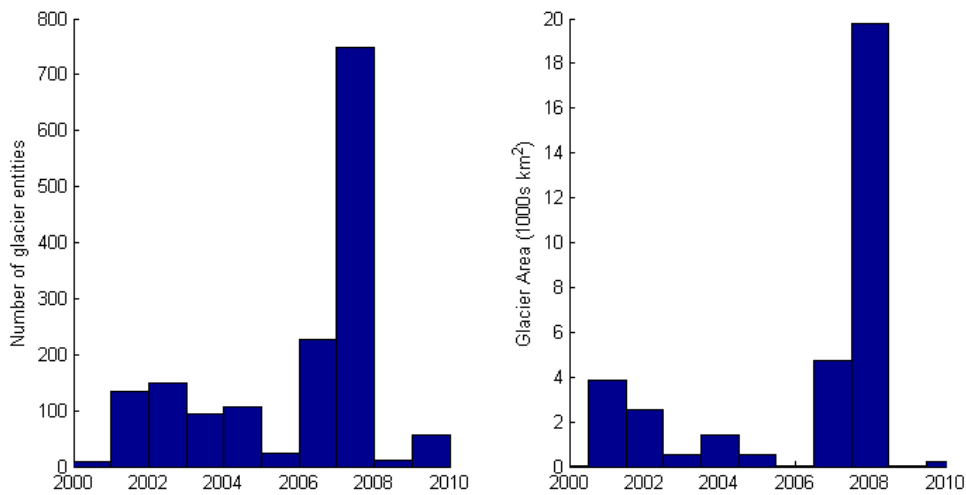
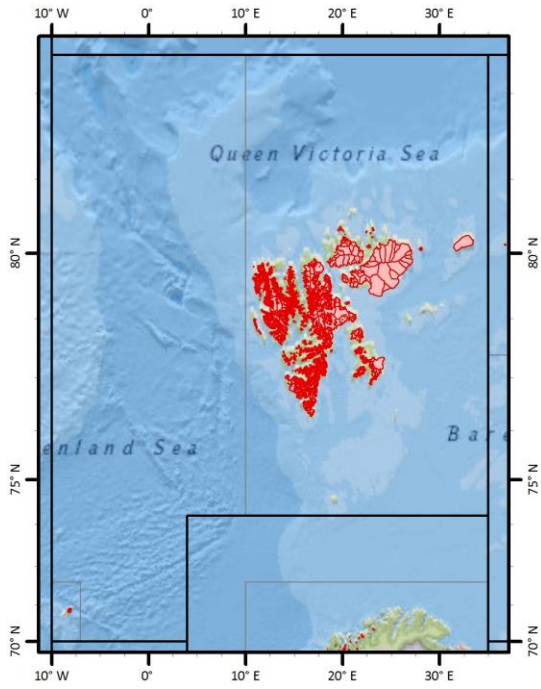


Figure 5. Time distribution of the imagery used to generate the Svalbard portion (region 07) of the RGI, showing the number of glaciers (left) and the total glacier area (right) as a function of image year.



5.8 REGION 8: Scandinavia

Contributor	Institution	Project/Funding
Andreassen, L.M. Hausberg, J.E. Winsvold, S.	Norwegian Water Resources and Energy Directorate (NVE), Norway	CryoClim/Norwegian Space Centre
Paul, F.	University of Zürich, Switzerland	GlobGlacier/ESA
Mercer, A. Brown, I.	University of Stockholm, Sweden	

Changes from Version 5.0 to 6.0

Exact dates were obtained for Norwegian glaciers from information submitted to GLIMS by L.M. Andreassen after the release of RGI version 1.0; see Andreassen et al., 2012. A further 885 glaciers, mostly small, were added from the same source. The Swedish and Norwegian parts of Salajekna (RGI60-08.03553), area 26.8 km², were merged.

The source for hypsometry was changed from the ASTER GDEM2 to the ViewfinderPanoramas DEM3 (<http://www.viewfinderpanoramas.org/>).

Changes from Version 4.0 to 5.0

Links were added to 24 glaciers in the WGMS mass-balance database.

Changes from Version 3.2 to Version 4.0

Four exterior *GLIMS*IDs were replaced. Topographic and hypsometric attributes (section 3.2) were added.

Changes from Version 3.0 to 3.2

None.

Changes from Version 2.0 to 3.0

Glaciers were delineated from glacier complexes.

Changes from Version 1.0 to Version 2.0

Four glaciers in the Khibiny Mountains of the Kola Peninsula (08-02) were added as nominal circles from WGI-XF.

Version 1.0

The glacier outlines for Norway are based on Landsat (TM and ETM+) imagery from 1999-2006.

The Swedish glacier outlines use imagery from SPOT5 and SPOT4 (dates not provided). In some regions these outlines were updated against September 2008 Swedish Land Survey imagery available on Google Earth.

The glacier mapping to which GlobGlacier contributed is documented in Andreassen et al. (2008) for Jotunheimen, Paul and Andreassen (2009) for Svartisen, and Paul et al. (2011) for the Jostedalbreen region.



5.9 REGION 9: Russian Arctic

Contributor	Institution	Project/Funding
Moholdt, G.	University of Oslo, Norway	ice2sea/grant number 226375

Changes from Version 5.0 to 6.0

The source for hypsometry was changed from the ASTER GDEM2 to the ViewfinderPanoramas DEM3 (<http://www.viewfinderpanoramas.org/>).

Changes from Version 4.0 to Version 5.0

Four glaciers (RGI50-09.00498, RGI50-09.00515, RGI50-09.00967, RGI50-09.00968) on October Revolution Island, Severnaya Zemlya, formerly with *TermType* = 1, were given the *TermType* code 5 because they flow into the Matushevich Ice Shelf.

Changes from Version 3.2 to Version 4.0

Topographic and hypsometric attributes (section 3.2) were added.

Changes from Version 3.0 to 3.2

None.

Changes from Version 2.0 to 3.0

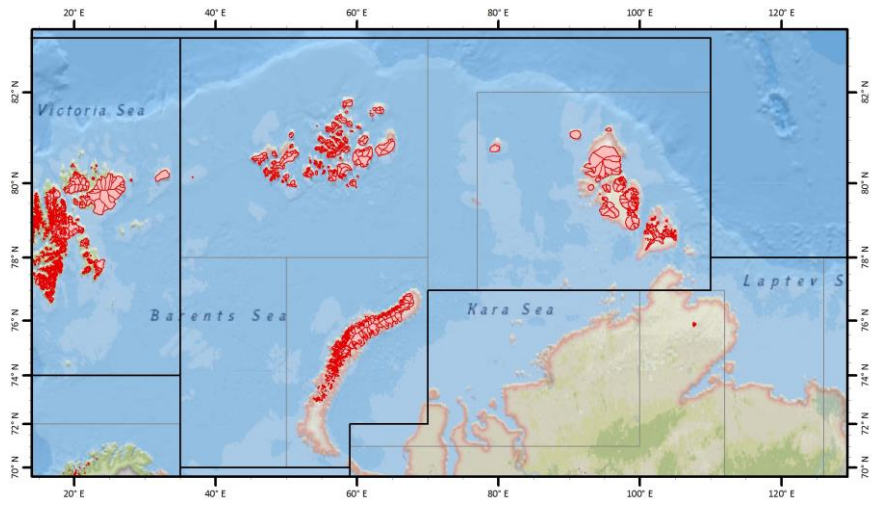
None.

Changes from Version 1.0 to Version 2.0

The Matushevich Ice Shelf, which was the only ice shelf in the inventory, was removed.

Version 1.0

The inventory was constructed as part of a mass balance study of the Barents/Kara Sea region (Moholdt et al., 2012). It covers all glaciers and ice caps in Novaya Zemlya (22,100 km²), Severnaya Zemlya (16,400 km²), Franz Josef Land (12,700 km²), Ushakov Island (320 km²) and Victoria Island (6 km²). Glacier complexes were manually digitized from orthorectified satellite imagery acquired during summers between 2000 and 2010. SPIRIT SPOT5 scenes (Korona et al., 2009) were used for most of Novaya Zemlya, while the best available Landsat scenes were used elsewhere. All visible nunataks were cut out from the glacier polygons, and snowfields were only included if they seemed to be a part of a glacier. Ice shelves in Franz Josef Land (<50 km²) were included as parts of the glacier polygons, while the Matushevich Ice Shelf in Severnaya Zemlya (~200 km²) was delineated into a separate polygon. The estimated total glacier area of the region (51,500 km²) is 9% smaller than that of the World Glacier Inventory (Ohmura, 2009). This large deviation is probably due to a combination of long-term glacier retreat and methodological differences in glacier delineation.



5.10 REGION 10: North Asia

Contributor	Institution	Project/Funding
L. Earl A.S. Gardner	Graduate School of Geography, Clark University, Worcester, MA; Jet Propulsion Laboratory, California Institute of Technology, Pasadena, CA	

Changes from Version 5.0 to 6.0

For some glaciers the source for hypsometry was changed from the ASTER GDEM2 to the ViewfinderPanoramas DEM3 (<http://www.viewfinderpanoramas.org/>).

An error in the minimum elevation of 11 glaciers was detected. It had been set wrongly to 0 and that value was reset to missing. The corresponding hypsometric lists were also set to missing.

Changes from Version 4.0 to 5.0

The inventory of mainland North Asia was replaced in its entirety from Earl and Gardner (2016). Nominal glaciers remain on Wrangell Island (3 km²) and the De Long Islands (Jeanette, Henrietta, Bennet; 81 km²). Glaciers in Chukotka (regions 10-05 and 10-06; Sedov 1997) that formerly appeared only in the RGI global grid are represented explicitly in version 5.0.

Glacier outlines retired from version 4.0 will be added to GLIMS if they are not in GLIMS already.

Links were added to 12 glaciers in the WGMS mass-balance database.

The four second-order regions of earlier RGI versions were replaced by six regions conforming to those of Earl and Gardner (2016). The outlines of the two sets of regions differ in detail, but all glaciers are in the same region in both the source and the RGI.

Changes from Version 3.2 to Version 4.0

One exterior *GLIMS*id was replaced. Topographic and hypsometric attributes (section 3.2) were added, although this could not be done for most glaciers in North Asia, of which 2,832 out of 4,403 are nominal glaciers.

The addition of dates for glaciers in the Chinese Altay is described under Region 13: Central Asia.

Changes from Version 3.0 to 3.2

None.

Changes from Version 2.0 to Version 3.0

All of the glaciers represented as circles were regenerated from WGI-XF (Cogley 2009). Some of them have not just nominal shapes but nominal positions, being derived from the Soviet *Katalog Lednikov*, which in each drainage basin gives full information only for glaciers larger than 0.1 km². Only a total number and total area are given for glaciers smaller than 0.1 km². In WGI-XF these small glaciers are all assigned a common position roughly in the centre of their basins, and an equal share of the listed small-glacier area. Obviously these and other nominal glaciers should not be used for purposes other than calculating total glacierized area.

Some DCW outlines were found to overlie mountain ranges whose ice cover was already represented by nominal glaciers. These duplicate DCW outlines were removed.

Changes from Version 1.0 to Version 2.0

The DCW outlines of glacier complexes in Mongolia were replaced by outlines of glaciers digitized by J.G. Cogley from Soviet military maps. Their dates range between 1968 and 1983.

14 glaciers in the Tajonos Peninsula, northwest of Kamchatka (10-02) were added as nominal circles from WGI-XF.

Version 1.0

About one third of the glacier outlines in North Asia were manually delineated from Landsat TM/ETM+ or ASTER imagery. Missing areas were filled by a glacier layer compiled by B. Raup (Raup et al., 2000) from the Digital Chart of the World (DCW) and the World Glacier Inventory (WGMS, 1989; Haeberli et al., 1998).

5.11 REGION 11: Central Europe

Contributor	Institution	Project/Funding
Frey, H. LeBris, R. Paul, F.	University of Zürich, Switzerland	GlobGlacier/ESA
R. Marti	Université de Toulouse, France	
A. Rabatel	Université de Grenoble Alpes, France	
C. Smiraglia G. Diolaiuti	Università degli Studi di Milano, Italy	

Changes from Version 5.0 to 6.0

The nominal glaciers in France and Italy, added in version 5.0, were replaced from Gardent et al. (2014; outlines from 2003) and Smiraglia et al. (2015; outlines from 2005–2012).

Changes from Version 4.0 to Version 5.0

The 108 nominal glaciers in the Pyrenees were replaced by 31 glaciers (representing late 2011) from a recent inventory by Renaud Marti, Université de Toulouse. The location (*GLIMSId*, *CenLon*, *CenLat*) of Gh del Calderone in the Appennines was corrected; its outline was added from a map in Gellatly et al. (1994a). Six glacierets in the Maritime Alps (Gellatly et al., 1994b), two in Slovenia (Triglav Čekada et al., 2012), one in Montenegro (Hughes 2008) and two in Albania (Milivojević et al., 2008) were added, the outlines being taken from maps in the source publications. Some Balkan ice bodies documented in these sources and in Grunewald et al. (2006) were not assimilated because they were smaller than the RGI threshold of 0.01 km².

The Bavarian glaciers were added from Hagg et al. (2012).

51 nominal glaciers in the Maritime and Cottian Alps (France and Italy) and 67 nominal glaciers in the Dolomitic Alps (Italy) were added from WGI-XF (Cogley, 2009).

Links were added to 31 glaciers in the WGMS mass-balance database.

Changes from Version 3.2 to Version 4.0

Five exterior *GLIMSIds* were replaced. Topographic and hypsometric attributes (section 3.2) were added.

Changes from Version 3.0 to 3.2

None.

Changes from Version 2.0 to 3.0

None.

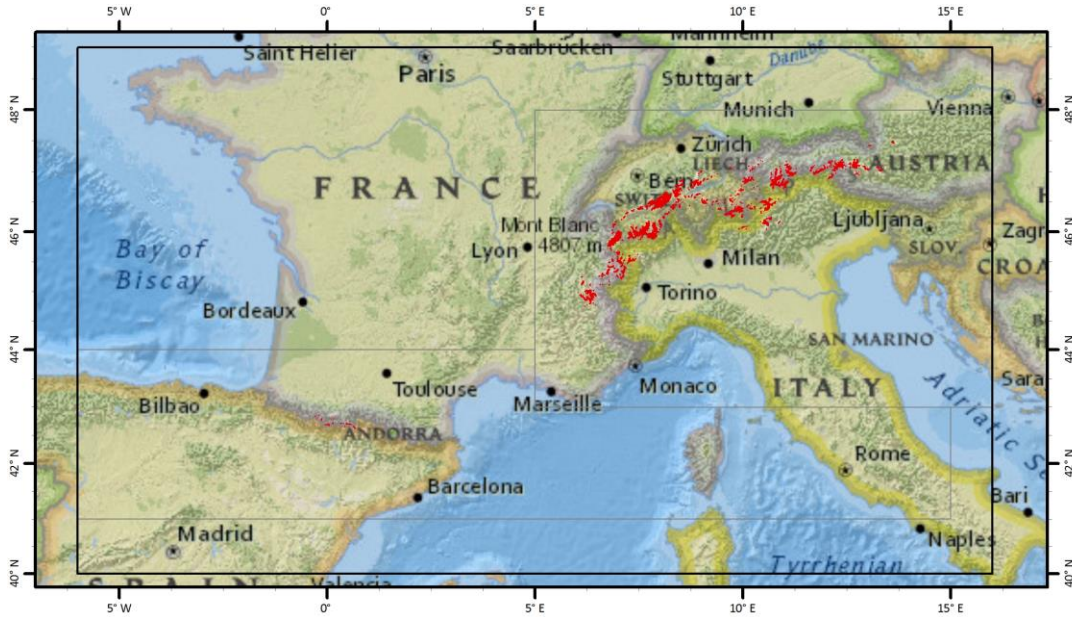
Changes from Version 1.0 to Version 2.0

109 glaciers in the Pyrenees, and one in the Appennines, were added as nominal circles from WGI-XF. Together they constitute region 11-02.

Version 1.0

The glacier outlines for this region are derived from ten Landsat TM images acquired during two months in the summer of 2003 using band-ratio images. Drainage divides for individual glaciers were derived from the void-filled SRTM DEM (from CGIARS) in a resampled version with 60 m spatial resolution. All further details are documented in Paul et al. (2011b). About 30-50 km² of glaciers are not mapped, mainly very small glaciers located in Italy (Brenta and Dolomites) and Germany, covered by debris or located under local orographic clouds. The original data sets (in UTM projection) can be downloaded from

<http://globglacier.ch/content.html?menuItem=sub5&contentItem=statusDataAccess> .



5.12 REGION 12: Caucasus and Middle East

Contributor	Institution	Project/Funding
Khromova, T.	Institute of Geography, Russian Academy of Science, Moscow, Russia	
N. Karimi	Ministry of Energy, Teheran, Iran	

Changes from Version 5.0 to 6.0

The 37 nominal glaciers in Iran, derived from Moussavi et al. (2009), were replaced by 200 glacier outlines submitted to GLIMS by Neamat Karimi (Ministry of Energy, Teheran).

Changes from Version 4.0 to 5.0

Links were added to 7 glaciers in the WGMS mass-balance database.

Changes from Version 3.2 to Version 4.0

One exterior *GLIMS*id was replaced. Topographic and hypsometric attributes (section 3.2) were added.

As noted by Shahgedanova et al. (2014), version 3.2 omitted glaciers in the western and eastern Greater Caucasus. These omissions have been partly rectified by adding nominal glaciers from WGI-XF (Cogley, 2009). The 339 added glaciers, with date ranges 1965–1976, cover 155 km² and also include some in the central Greater Caucasus (on the Svanets and Lechkhum Ranges to the south of the main ridge of the Caucasus) and in the Lesser Caucasus in Armenia.

Changes from Version 2.0 to 3.0

None.

Changes from Version 2.0 to 3.0

Outlines of the glaciers of Turkey were provided by M.A. Sarıkaya (Sarıkaya and Tekeli, 2013).

Changes from Version 1.0 to Version 2.0

The 37 glaciers of Iran (12-02) were added as nominal circles from Moussavi et al. (2009). The information available for Turkey (Kurter 1991) was not adequate for placing the individual glaciers, which have a total area of 22.9 km².

Version 1.0

Outlines of glaciers in the Caucasus were obtained from the GLIMS database (Raup et al., 2007).



5.13 REGION 13: Central Asia

Contributor	Institution	Project/Funding
Bolch, T. Mölg, N. Frey, H. Paul, F.	Technical University of Dresden, Germany; University of Zürich, Switzerland	DynRG-TiP, Aksu-Tarim-RS/ German Research Foundation (DFG) Glaciers_cci/ESA
W.Q. Guo S.Y. Liu	Cold and Arid Regions Environmental and Engineering Research Institute, Lanzhou, China	Grants 2006FY110200, 2013FY111400/ Ministry of Science and Technology Grants KZCX2-YW-301, KZCX2-YW- GJ04/Chinese Academy of Sciences
Nuimura, T. Sakai, A.	University of Nagoya	NEXT Program, GR052/ Japan Society for the Promotion of Science, 26257202,

Changes from Version 5.0 to 6.0

None.

Changes from Version 4.0 to 5.0

Regions 13, 14 and 15 are entirely new in version 5.0. being taken from Nuimura et al. (2015), Guo et al. (2015) and as-yet unpublished work at the Technical University of Dresden and University of Zürich. The Dresden/Zürich outlines cover the Karakoram in region 14.

The GAMDAM inventory of Nuimura et al. (2015) covers all of High Mountain Asia (including RGI region 10-04). The Second Chinese Glacier Inventory (CGI2) of Guo et al. (2105) covers China. The GAMDAM outlines are nearly all from 1999–2003 and thus conform with the recommendation of Paul et al. (2009) to select imagery as close to 2000 as possible. However they exclude thin ice on headwalls and tend to have areas smaller than those measured in conformance with GLIMS guidelines (Raup and Singh Khalsa, 2007). The CGI2 inventory has outlines mostly from a target period of 2006–2010, but includes older outlines from the First Chinese Glacier Inventory (CGI1) where suitable imagery could not be found within the target period.

A final decision about selection for the RGI from these extensive sources awaits detailed intercomparison. RGI version 5.0 incorporates those CGI2 outlines that are not from CGI1, and GAMDAM outlines in areas of remaining CGI1 coverage as well as areas outside China other than the Karakoram.

Glacier outlines retired from version 4.0 will be added to GLIMS if they are not in GLIMS already.

Links were added to 17 glaciers in the WGMS mass-balance database.

Changes from Version 3.2 to Version 4.0

45 exterior *GLIMS*IDs were replaced. Topographic and hypsometric attributes (section 3.2) were added.

An effort was made to recover as many dates as possible for High Mountain Asia as a whole. Duplication was avoided by creating disjunct polygons for each source, including the Chinese Glacier Inventory (CGI). The outlines of most RGI glaciers on Chinese territory were obtained from

the GLIMS database before the RGI system of attributes was adopted. Some of the other sources of dates for High Mountain Asia were partly on Chinese territory.

The dates of CGI glaciers were recovered from the 24 May 2011 version of GLIMS. The CGI and RGI outlines were matched by computing arc distances between their *GLIMSId* locations. Because some work was done for the RGI on correcting mislocated CGI glaciers, this operation was not straightforward. By inspection of trial results, and bearing in mind that the aim was only to place the glacier within the outline of its source image or air photograph, a separation not exceeding 2 km was found sufficient to assign the CGI date accurately to its closest RGI counterpart. Of 50,458 glaciers within the CGI polygon, 38% had exactly matching locations, 43% had separations within 300 m, and 1.4% (709) failed the 2-km test of proximity. Thus the CGI yielded 37,769 new dates, covering 53,192 km², for RGI 4.0.

The glacier inventory of the Nyainqentanghla Range in southeastern Tibet by Bolch et al. (2010b) was one of the sources for RGI 3.2, and the necessary dates for 789 glaciers (area 796 km²) were recovered from that paper. The mountain range was subdivided into three dated polygons, each representing a different source image or set of images.

Most of the *O2Region* codes in earlier versions were incorrect and have been corrected.

Where Chinese RGI glaciers could be matched with confidence to their equivalents in GLIMS, their 12-character WGI identification codes (modified after Müller et al., 1978) were added to the *Name* field.

Changes from Version 3.0 to Version 3.2

None

Changes from Version 2.0 to Version 3.0

Glacier outlines in much of the central Tien Shan were replaced by the inventory of Osmonov et al. (2013). The outlines were mapped semi-automatically and manually based on Landsat TM data from ~2008. This inventory is superior to the former data as the geolocation is correct while the other data obtained from the GLIMS data base had inhomogeneous shifts. In the Pamir, several outlines from the DCW were replaced by semi-automatically mapped outlines based on Landsat TM/ETM+ data from ~2000. The large offset between the GLIMS data and data from the CGI in eastern Pamir was reduced..

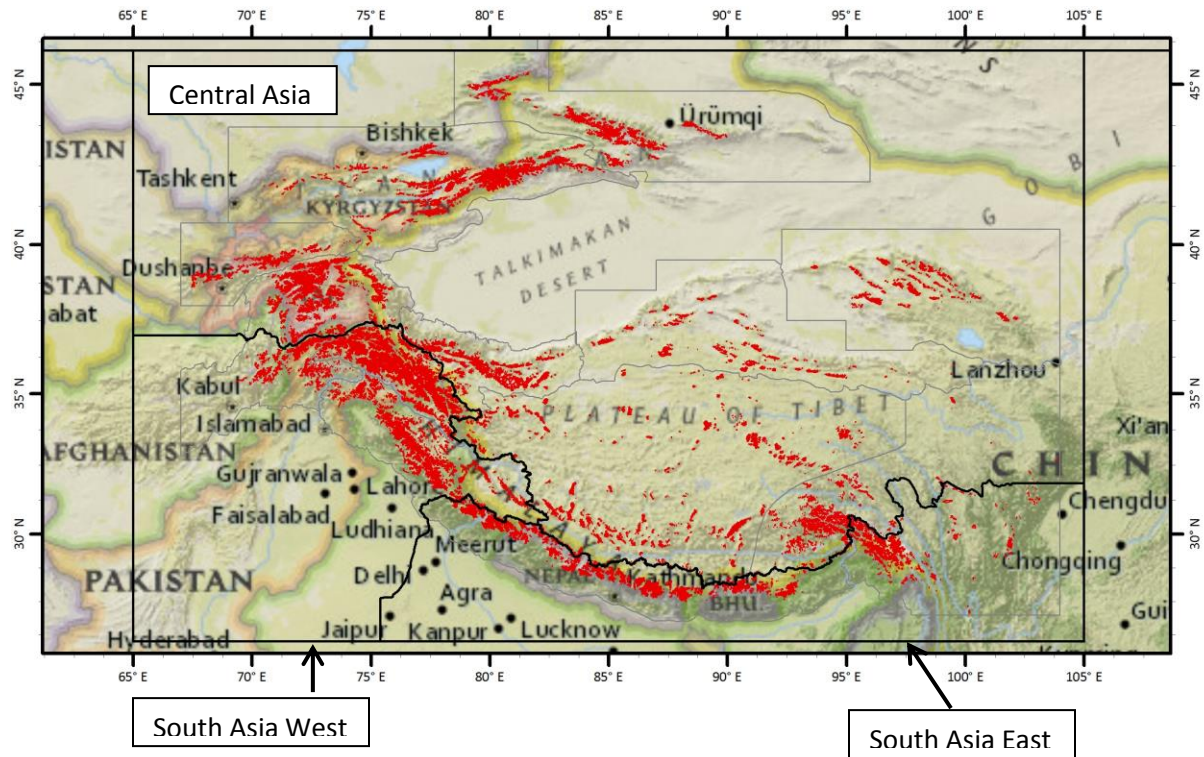
Changes from Version 1.0 to Version 2.0

None.

Version 1.0

Large parts of Central Asia are covered by the GLIMS database, which consists in China of data from the first Chinese Glacier Inventory (Shi et al., 2009) and is of heterogeneous and generally slightly lower quality (more generalized) than the other glacier data used here. It has also to be noted that some of the GLIMS data in Central Asia have a shift in location. Large parts of the Tien Shan in Kazakhstan and Kyrgyzstan were mapped manually or semi-automatically using ratio images from ASTER and Landsat data (e.g. Kutuzov and Shahgedanova, 2009; Kriegel et al., 2013). Important missing areas such as the Central Pamirs, Naryn basin, northern Tien Shan (Bolch, 2007) and the Dzhungarian Alatau were mapped semi-automatically with manual corrections using Landsat TM/ETM+ scenes. The glacier inventory for the Nyainqentanghla Range in Tibet was taken from Bolch et al. (2010b).

Remaining missing areas were filled by a glacier layer compiled by B. Raup (Raup et al., 2000) from the Digital Chart of the World (DCW) and the World Glacier Inventory (WGMS, 1989; Haerberli et al., 1998). The DCW outlines are in western Kyrgyzstan (region 13-03), the Hissar Alay (13-01), the Safed Khirs (northern Afghanistan) and parts of the southwest Pamir (13-02).



5.14 REGION 14: South Asia West

Contributor	Institution	Project/Funding
Bolch, T. Frey, H. Paul, F.	University of Zürich, Switzerland	GlobGlacier/ESA Glaciers_cci/ESA
W.Q. Guo S.Y. Liu	Cold and Arid Regions Environmental and Engineering Research Institute, Lanzhou, China	Grants 2006FY110200, 2013FY111400/ Ministry of Science and Technology Grants KZCX2-YW-301, KZCX2-YW-GJ04/Chinese Academy of Sciences
Nuimura, T. Sakai, A.	University of Nagoya	NEXT Program, GR052/ Japan Society for the Promotion of Science, 26257202,

Changes from Version 5.0 to 6.0

None.

Changes from Version 4.0 to 5.0

Regions 13, 14 and 15 are entirely new in version 5.0. being taken from Nuimura et al. (2015), Guo et al. (2015) and as-yet unpublished work at the Technical University of Dresden and University of Zürich.

The Dresden/Zürich outlines cover the Karakoram in region 14. All were adopted for RGI version 5.0. Parts of region 14 not covered by this source were taken from the Second Chinese Glacier Inventory (CGI2) of Guo et al. (2015), and from the GAMDAM inventory of Nuimura et al. (2015) in areas outside the coverage of CGI2.

Glacier outlines retired from version 4.0 will be added to GLIMS if they are not in GLIMS already.

Links were added to 3 glaciers in the WGMS mass-balance database.

Changes from Version 3.2 to Version 4.0

36 exterior *GLIMSids* were replaced. Topographic and hypsometric attributes (section 3.2) were added.

Dates were added from two regional inventories that were sources for RGI 3.2. A *BgnDate* of 2 August 2002 was assigned to 1,184 glaciers (area 3,118 km²) in the basin of the upper Shyok River (Bhambri et al., 2013). Dates for 11,531 glaciers (area 9,124 km²) in northwestern India (Frey et al., 2012) were recovered by comparing the GLIMS version of the inventory with the RGI 3.2 version, matching glaciers by their *GLIMSids*, and transferring the dates from the GLIMS version.

Elsewhere in the Himalayan range, most of the RGI glacier outlines are from reports of the International Centre for Integrated Mountain Development (ICIMOD). Polygons were generated to enclose the glaciers inventoried by Sah et al. (2005) in Uttarakhand and by Mool et al. (2005) in northern Pakistan and the upper Indus basin. The RGI 3.2 glaciers within each polygon were

assigned the date of the corresponding image, verified by comparison with the glacier-by-glacier lists in the source.

See Region 13: Central Asia for the recovery of dates for Chinese glaciers. Where RGI glacier outlines from the first Chinese Glacier Inventory could be matched with confidence to their equivalents in GLIMS, their 12-character WGI identification codes (modified after Müller et al., 1978) were added to the *Name* field.

Changes from Version 3.0 to Version 3.2

None.

Changes from Version 2.0 to Version 3.0

None.

Changes from Version 1.0 to Version 2.0

Six glaciers in the Ghorband River basin, Afghanistan (region 14-01) were added as nominal circles from WGI-XF. The Ghorband is one of the headwaters of the Kabul River and thus of the Indus. It is possible that more Afghan glaciers remain to be identified further to the southwest (Shroder and Bishop 2010).

Version 1.0

Large parts of the Himalaya and Karakoram are covered by the GLIMS database (Raup et al., 2007), to which they were originally contributed by T. Khromova. For the RGI, GLIMS was used as the source where no other was available, mainly on the northern slopes of the Himalayas and the northeastern part of the Karakoram. In these regions, the GLIMS database consists mostly of data from the first Chinese Glacier Inventory (Shi et al., 2009) and is of heterogeneous and generally slightly lower quality than the other glacier data used here. Glacier outlines compiled by ICIMOD were used for parts of the Karakoram (Mool et al., 2007). The outlines in the Shyok River basin (northeastern Karakoram) are from Bhambri et al. (2013). For parts of northwestern India, glacier inventory data compiled by the GlobGlacier project of the European Space Agency (ESA) (Paul et al., 2009) was used; the information was compiled from Landsat ETM+ and ALOS PALSAR data (Frey et al., 2012). For a few regions in the Karakoram, no suitable glacier data was available. We therefore compiled new glacier outlines in these regions based on Landsat ETM+ data from the years 2002, 2009, and 2010.

5.15 REGION 15: South Asia East

Contributor	Institution	Project/Funding
W.Q. Guo S.Y. Liu	Cold and Arid Regions Environmental and Engineering Research Institute, Lanzhou, China	Grants 2006FY110200, 2013FY111400/ Ministry of Science and Technology Grants KZCX2-YW-301, KZCX2-YW-GJ04/Chinese Academy of Sciences
Nuimura, T. Sakai, A.	University of Nagoya	NEXT Program, GR052/ Japan Society for the Promotion of Science, 26257202,

Changes from Version 5.0 to 6.0

None.

Changes from Version 4.0 to 5.0

Regions 13, 14 and 15 are entirely new in version 5.0. being taken from Nuimura et al. (2015), Guo et al. (2015) and as-yet unpublished work at the Technical University of Dresden and University of Zürich. The Dresden/Zürich outlines do not cover region 15.

The GAMDAM inventory of Nuimura et al. (2015) covers all of High Mountain Asia (including RGI region 10-04). The Second Chinese Glacier Inventory (CGI2) of Guo et al. (2015) covers China and Arunachal Pradesh. The GAMDAM outlines are nearly all from 1999–2003 and thus conform with the recommendation of Paul et al. (2009) to select imagery as close to 2000 as possible. However they exclude thin ice on headwalls and in that sense are not in conformance with GLIMS guidelines (Raup and Singh Khalsa, 2007). The CGI2 inventory has outlines mostly from a target period of 2006–2010, but includes older outlines from the First Chinese Glacier Inventory (CGI1) where suitable imagery could not be found within the target period.

A final decision about selection for the RGI from these extensive sources awaits detailed intercomparison. RGI version 5.0 incorporates those CGI2 outlines that are not from CGI1, and GAMDAM outlines in areas of remaining CGI1 coverage as well as areas outside China.

Glacier outlines retired from version 4.0 will be added to GLIMS if they are not in GLIMS already.

Links were added to 5 glaciers in the WGMS mass-balance database.

Changes from Version 3.2 to Version 4.0

Nine exterior *GLIMS* IDs were replaced. Topographic and hypsometric attributes (section 3.2) were added.

Dates were recovered for as many glaciers as possible. For Bhutan, a polygon enclosing the glaciers inventoried by Mool et al. (2001) was created and subdivided into three polygons, one for each of the image sets from which the glaciers were identified. The RGI 3.2 glaciers within each polygon were assigned the date of the corresponding image, verified by comparison with the glacier-by-glacier lists in the source. Equivalent procedures were adopted for Sikkim (Mool et al., 2003) and the basins of the Pum (upper Arun; Wu et al., 2003) and Poi and Rongxer (upper Bhote–Sun Koshi and Tama Koshi; Wu et al., 2004) rivers. Glaciers elsewhere in Nepal were assigned a date range from 2008 to 2009 (ICIMOD, 2011a,b), consistent with those in earlier versions.

See Region 13: Central Asia for the recovery of dates for Chinese glaciers. Where RGI glacier outlines from the first Chinese Glacier Inventory could be matched with confidence to their equivalents in GLIMS, their 12-character WGI identification codes (modified after Müller et al., 1978) were added to the *Name* field.

Changes from Version 3.0 to Version 3.2

None.

Changes from Version 2.0 to Version 3.0

Outlines of the glaciers of Burma, provided by S. Bajracharya, were added.

Changes from Version 1.0 to Version 2.0

None.

Version 1.0

Large parts of the Himalaya are covered by the GLIMS database (Raup et al., 2007). For the RGI, GLIMS was used as the source where no other was available, mainly on the northern slopes of the Himalayas. In these regions, the GLIMS database consists mostly of data from the first Chinese Glacier Inventory (Shi et al., 2009) and is of heterogeneous and generally slightly lower quality than the other glacier data used here. Glacier outlines compiled by ICIMOD were used for the central and eastern Himalayas (Mool et al. 2007). For Nepal, more recent information from 2008 and 2009 is available and was used here (ICIMOD, 2011a,b).

5.16 REGION 16: Low Latitudes

Contributor	Institution	Project/Funding
Sharp, M. Wyatt, F.	University of Alberta, Canada	
Miles, E.	University of British Columbia, Canada	
Kienholz, C.	Uninversity of Alaska Fairbanks	

Changes from Version 5.0 to 6.0

Coverage of the glaciers of Cotopaxi, Ecuador, was replaced with outlines for 1997 digitized from Jordan et al. (2005).

Changes from Version 4.0 to 5.0

Links were added to 2 glaciers in the WGMS mass-balance database.

Changes from Version 3.2 to Version 4.0

94 exterior *GLIMS*Ids were replaced. Topographic and hypsometric attributes (section 3.2) were added.

The 81 remaining glacier complexes in the Bolivian Andes were subdivided by C. Kienholz into 159 glaciers. *RGI*Ids for the whole of region 16 were altered in consequence.

Changes from Version 3.0 to Version 3.2

Outlines of the glaciers of Mexico were replaced with outlines provided by E. Burgess, and the nominal glaciers of east Africa and New Guinea were replaced with outlines provided by N.J. Cullen and A. Klein respectively. Note that several glacier complexes are still present in southern Peru and western Bolivia.

Changes made from Version 2.0 to Version 3.0

Some outlines in northern Chile were improved.

Changes from Version 1.0 to Version 2.0

Outlines of the glaciers of Mexico (16-02) were digitized by J.G. Cogley from maps in White (2002). 59 glaciers in east Africa (16-03) and seven in New Guinea (16-04) were added as nominal circles from WGI-XF.

Summary of quality controls conducted by E.S. Miles, University of British Columbia:

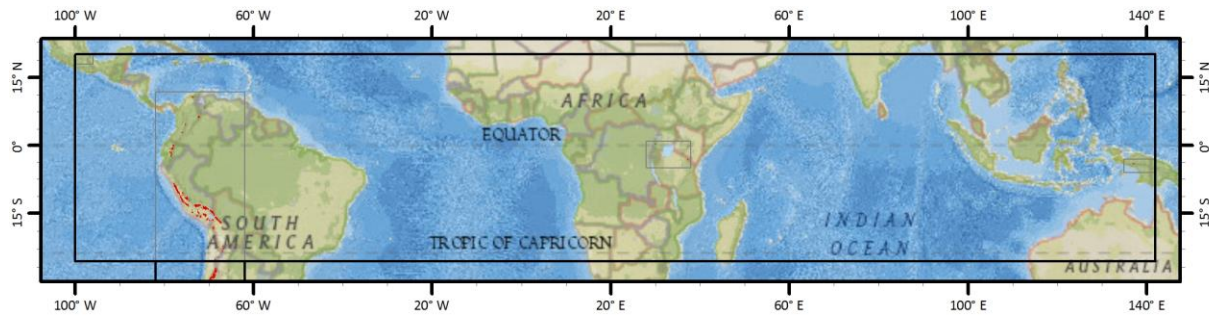
1. Version 1.0 RGI shapefile topology was corrected, splitting the complexes into glaciers (total of 14167 polygons).
2. Using the ice flowshed delineation script developed by C. Kienholz (UAF), the glacier polygons were divided into expected ice drainages. This processing preserved the original area of 5066.1 km² (measured in UTM 18S) and resulted in 16255 polygons.
3. All polygons smaller than 0.01 km² were then removed. A survey of these polygons showed that the vast majority were isolated and contained only 3 or 4 vertices. These small polygons (9869 in number) encompassed a total area of 20.8 km², again measured in UTM 18S.

4. The remaining 6386 polygons were individually inspected in ArcGIS with a standard ESRI satellite image basemap to remove gross inaccuracies.
 - 4.1. Due to difficulties in obtaining minimum-snow satellite imagery for the NDSI calculation used to create the initial dataset, there was significant snow contamination in the glacier dataset. The most obvious problems occurred in the severely arid regions of southern Peru and northern Chile, although problems were also evident in the temperate zones.
 - 4.2. Each polygon was inspected with consideration for the basemap satellite imagery, with scale fixed at 1:50,000 unless specific outlines warranted further inspection.
 - 4.2.1. Glacier outlines which were snow-covered or obscured by clouds in the basemap imagery were preserved as-is.
 - 4.2.2. Many glacier outlines encompassed both snow and rock (or vegetation, etc). If the snow portion was substantial (over a third or distributed over the entire outline), the outline was left as-is. If snow encompassed a very small and concentrated portion of the polygon, the polygon was roughly trimmed to this extent.
 - 4.2.3. Only glaciers containing no snow cover, where a debris-covered glacier was also implausible, were removed in their entirety.
 - 4.3. The resulting dataset included 4382 glacier outlines and 4088.2 km².
5. This inspection revealed an odd spatial shift for all polygons in a contiguous region between approximately Huaraz, Peru, and Conchucon, Peru. The features did not properly align with mountains evident in the ArcMap satellite imagery or in Google Earth. Most of the features appeared to be shifted by approximately 1.2km north of the mountains that they matched, and a zone near Huaraz had duplicate outlines – one set of glaciers mapping correctly over the mountains with a matching set of features located about 1.2 km to the north. Probably due to an incorrect spatial representation of one of the source images used in the original glacier demarcation, the misregistration would be problematic for modelling.
 - 5.1. All glacier outlines within this region were extracted from the entire dataset (and deleted from the original). Individually, each glacier complex was uniformly shifted approximately 1.2km south, then adjusted to provide the best fit with topography and the satellite imagery backdrop. Since the required transformation was not quite linear (more shift was required for the northernmost outlines) it is likely that the source image had some minor distortion associated with the misregistration.
 - 5.2. The duplicate features were then manually trimmed (coarsely) according to a combination of the two outlines available in conjunction with the satellite image backdrop.
 - 5.3. After a satisfactory shift had been imposed, the individual glacier outlines were merged to a single polygon, and re-run through C. Kienholz's ice flowshed delineation script, such that the outlines would represent ice divides according to the correct topography.
 - 5.4. The corrected outlines were then merged back into the larger dataset and seams were trimmed where the polygons intersected.
6. The resulting dataset contains a total of 4373 outlines and covers an area of 4057.1 km².
7. Inspection of all polygon suggests that a more rigorous examination and delineation of each glacier would result in a further area reduction of up to 20%. Many outlines extend well beyond the terminus implied by the available satellite imagery, but the objective was primarily to remove the outlines that obviously did not represent glaciers at all.

Version 1.0

Shapefiles were created from late-summer, cloud-free Landsat 7 ETM+ imagery acquired prior to the 2003 scan line corrector (SLC) failure. To identify glacier surfaces, a normalized difference

snow index (NDSI) was calculated using bands 5 and 2 for the red and near-infrared bands respectively. A threshold of approximately 0.5-0.65 was used to identify dirty/shady/bare ice, and one from 0.65-0.99 to identify snow-covered ice. Gridded files were then converted to polygons and additional manual editing was carried out to eliminate incorrectly classified regions.



5.17 REGION 17: Southern Andes

Contributor	Institution	Project/Funding
Sharp, M. Wyatt, F.	University of Alberta, Canada	
Miles, E.	University of British Columbia, Canada	
De Angelis, H.	Stockholm University, Sweden	
Mölg, N., Paul, F.	University of Zürich, Switzerland	Glaciers_cci/ESA

Changes from Version 5.0 to 6.0

Coverage of the North Patagonian Ice Field was replaced with outlines for 2001 (Rivera et al., 2007) obtained from GLIMS.

Names of glaciers in the North and South Patagonian Icefields were added.

Changes from Version 4.0 to 5.0

Links were added to 2 glaciers in the WGMS mass-balance database.

Changes from Version 3.2 to Version 4.0

68 exterior *GLIMS* IDs were replaced. Topographic and hypsometric attributes (section 3.2) were added.

Changes from Version 3.0 to Version 3.2

None.

Changes from Version 2.0 to Version 3.0

Substantial revisions were made by N. Mölg in central Chile (Paul and Mölg, 2014) and in the mountains surrounding the North and South Patagonian Icefields.

Changes from Version 1.0 to Version 2.0

Summary of quality controls conducted by E.S. Miles, University of British Columbia:

1. The original RGI shapefile's topology was corrected, splitting complexes into individual glaciers (total of 42,397 polygons covering 33786 km²).

2. All polygons smaller than 0.01 km² were then removed. A survey of these polygons showed that (as in the Low-latitude Andes) the vast majority were isolated and contained only 3 or 4 vertices. These small polygons (26,396 in number) encompassed a total area of 59.23 km².

2.1 The remaining 16,001 polygons were individually inspected in ArcGIS and compared to a standard ESRI satellite image basemap and a Bing Maps satellite basemap to remove gross inaccuracies. The Bing basemap was used primarily for areas where the ESRI image included substantial cloud cover. The two basemaps were qualitatively compared in cloud-free regions and the agreement was deemed satisfactory for the removal of blatantly erroneous data. For highly ambiguous zones, Google Earth was utilized as a third image and rough terrain dataset to help interpret the satellite images and glacier outlines.

2.2 Due to difficulties in obtaining minimum-snow satellite imagery for the NDSI calculation used to create the initial dataset, there was significant snow contamination in the glacier dataset. This problem was most evident in southern Patagonia. Outlines in the Cordillera Darwin and the ranges east of the Icefields often represented snowlines rather than glacier outlines. Additionally, debris-covered glaciers and water-terminating glacial tongues posed

significant problems for the NDSI algorithm. Finally, the utilization of Landsat-7 data inappropriately blended with Landsat-5 data led to substantial stripe patterns in some areas (different sampling dates resulted in a changed snowline between the striped L7 data and the solid L5 data).

2.3 Each polygon was inspected with consideration for the basemap satellite imagery, with scale fixed at 1:60,000 unless specific outlines warranted further inspection.

2.3.1 Glacier outlines which were snow-covered or obscured by clouds in all the basemap imagery were preserved as-is.

2.3.2 Many glacier outlines encompassed both snow and rock (or vegetation, etc). If the snow portion was substantial (over a third or distributed over the entire outline), the outline was left as-is. If snow encompassed a very small and concentrated portion of the polygon, the polygon was roughly trimmed to this extent.

2.3.3 Striping due to L5/L7 blending was edited where possible.

2.3.4 Many glacier outlines included peripheral zones that were implausible as connected zones of deforming ice, but realistically could include glacierets or other perennial ice cover. These zones were eliminated where possible, but were often left in the dataset.

2.3.5 Only glaciers where there was no snow cover and a debris-covered glacier was also implausible (lakes, vegetated slopes, snow-banked streams, etc.) were removed in their entirety.

2.3.6 Water-terminating glacier tongues were often enlarged to cover the extent shown in the satellite imagery. Debris exposed as the tongue melts seemed to frustrate the algorithm. The same problem arose with larger land-terminating glaciers whose tongues had accumulated significant debris.

2.3.7 Debris-covered glaciers were in some cases omitted in their entirety by the dataset. About 20-25 rough outlines of such glaciers were added, based on inspection of the three imagery datasets. Most were between 33.5 and 34.5 degrees South.

2.4 The resulting dataset included 14,014 glacier outlines.

3. The next step was to incorporate the glacier outlines for the Lagos region of Chile and Argentina, developed by F. Paul.

3.1 The extent of the source scenes was not perfectly clear, but F. Paul's dataset was assumed to cover region 17 in its entirety.

3.2 At the southern margin of this dataset, two glacier outlines had straight-line southern edges. They were assumed to be outlines falling on the satellite image's edge, and corresponded directly to RGI outlines that continued further south. These overlapping outlines were combined.

4. The combined dataset (edited RGI and F. Paul's outlines) was then processed with C. Kienholz's flowshed delineation algorithm.

5. The next step was to incorporate H. De Angelis' outlines for the South Patagonian Icefield.

5.1 All outlines that intersected the prior-version South Patagonian Icefield polygon (which blended into adjacent ranges due to snowline outlines) were extracted from the recently-edited dataset.

5.2 These outlines were then intersected with the De Angelis outlines, creating a combined dataset containing outlines split by flowsheds. These polygons were examined individually with respect to the same basemaps identified above.

5.2.1 De Angelis polygons were left as-is.

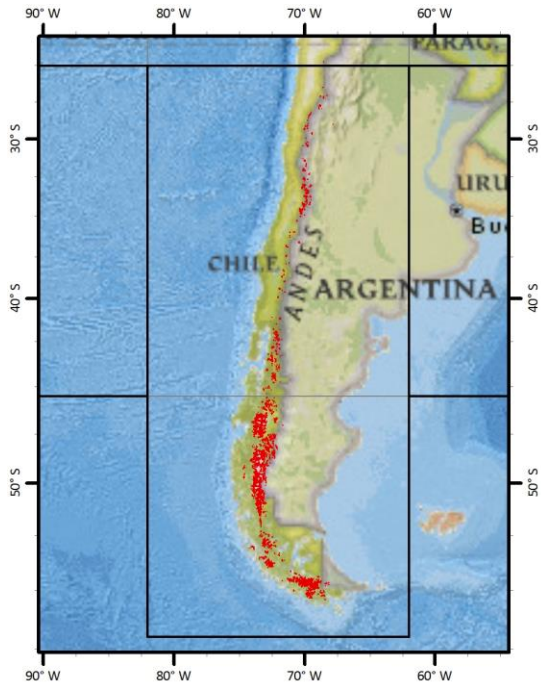
5.2.2 Polygons which appeared separated from the icefield were left as-is.

- 5.2.3 Exception: Sliver polygons removed from the icefield were removed when it was clear that editing had not produced a realistic flowshed.
- 5.2.4 Polygons adjacent to the icefield were included when the appearance of the basemap suggested an independent flowshed.
- 5.2.5 Polygons adjacent to the icefield were sometimes thin slivers (the recently-edited extent differed from the De Angelis extent), which were removed.
- 5.3 This dataset was then merged with the F. Paul and edited RGI outlines described above.
6. The final dataset contained 17,438 glacier outlines, covering a total area of 32,558 km².
- 6.1 While the Southern Andes only exhibited a change of 1000km² of coverage as the result of this editing, the improvements were much more extensive than for the Low-latitude Andes.
- 6.2 Substantial reductions in area due to the elimination of false-positive area (lakes, snow, or vegetation cover included in glacier outlines) were largely offset by inclusion of false-negative area (debris-covered glaciers and water-terminating tongues). Via intermediate datasets it can be estimated that more than 2000km² of false-positive area were eliminated before the inclusion of 1000km² of false-negative area.
- 6.3 Where they were possible, eliminations of area led to much more realistic glacier outlines, rather than a fractured landscape. There are still substantial gains to be made in this realm, but those gains would require much more extensive efforts.
- 6.4 An estimated 5% error by area remains in the dataset, mostly as glacier-peripheral snow and transient ice, which is clearly evident in examination of the outlines. Since one connected ice mass (the North Patagonian Icefield) contains ~50% of the region's ice area, peripheral areas are minor on a percent-areal basis, but may amount to hundreds of km².
- 6.5 This dataset is assessed on the whole as yielding a conservative area estimate, having accounted for nearly all of the false-negative zones.

Version 1.0

Shapefiles were created from late-summer, cloud-free Landsat 7 ETM+ imagery acquired prior to the 2003 SLC failure. To identify glacier surfaces, a normalized difference snow index (NDSI) was calculated using bands 5 and 2 for the red and near-infrared bands respectively. A threshold of approximately 0.5-0.65 was used to identify dirty/shady/bare ice, and one from 0.65-0.99 to identify snow-covered ice. Gridded files were then converted to polygons and additional manual editing was carried out to eliminate incorrectly classified regions.

Shapefiles for the South Patagonian Icefield were provided by H. De Angelis (De Angelis, 2014).



5.18 REGION 18: New Zealand

Contributor	Institution	Project/Funding
Chinn, T.	Canterbury University, NZ	

Changes from Version 5.0 to 6.0

None.

Changes from Version 4.0 to 5.0

Links were added to 4 glaciers in the WGMS mass-balance database.

Changes from Version 3.2 to Version 4.0

89 exterior *GLIMS*ids were replaced. Topographic and hypsometric attributes (section 3.2) were added.

Changes from Version 3.0 to Version 3.2

None.

Changes from Version 2.0 to Version 3.0

Glaciers were delineated from glacier complexes.

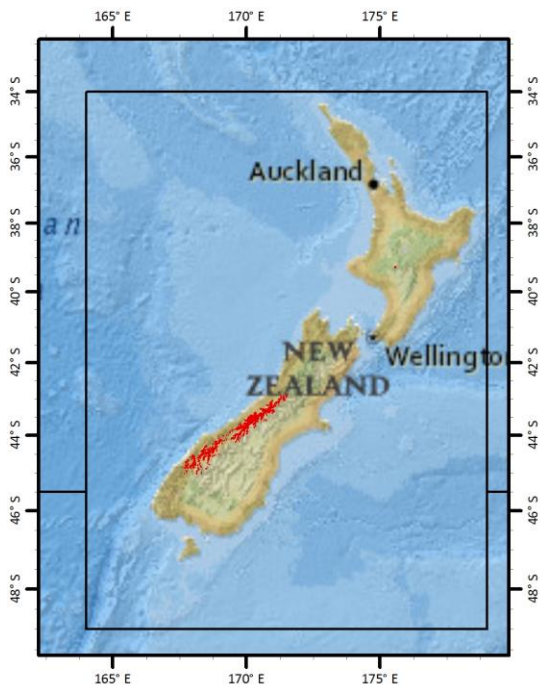
Changes from Version 1.0 to Version 2.0

None.

Version 1.0

New Zealand outlines are derived from 1978 aerial imagery at a scale of 1:150,000 as used for the NZ Topo50 maps (Chinn, 2001). The shapefile can be downloaded from:

<http://data.linz.govt.nz/#/layer/287-nz-mainland-ice-polygons-topo-150k/>



5.19 REGION 19: Antarctic and Subantarctic

Contributor	Institution	Project/Funding
Bliss, A.	University of Alaska, Fairbanks, USA	National Science Foundation (US)
LeBris , R. Berthier, E.	CNRS-OMP-LEGOS, France	French Space Agency (CNES)
Cogley, J.G.	Trent University, Canada	
Paul, F.	University of Zürich, Switzerland	Glaciers_cci/ESA

Changes from Version 5.0 to 6.0

None.

Changes from Version 4.0 to 5.0

Links were added to 2 glaciers in the WGMS mass-balance database.

Changes from Version 3.2 to Version 4.0

Two exterior *GLIMS*IDs were replaced. Topographic and hypsometric attributes (section 3.2) were added.

The main source for RGI region 19 was the Antarctic Digital Database (ADD; ADD Consortium, 2000), compiled for glaciological purposes by Bliss et al. (2013). In RGI 3.2, 34,041 km² of Antarctic glaciers had dates and 47,961 km² had date ranges. Most of these were obtained from attributes of coastal and other line segments in the ADD. Of the remaining 50,866 km² of glaciers, it was possible to recover dates and date ranges for 35,148 km² from chapter 5 (Bibliography) of the ADD manual (ADD Consortium, 2000). This bibliography gives detailed summaries of ADD revisions organized by the tiles into which the database is subdivided, and further by the 16 maps into which each tile is subdivided. For many tiles, but not all, the bibliography lists source images and their dates. Unfortunately the bibliography has not been updated since 2000, and so there is some doubt about the assignment of dates. Often, however, it was possible to verify, for example by inspecting Google Earth, that there have been no perceptible revisions in recent years.

Changes from Version 2.0 to Version 3.2

None.

Changes from Version 2.0 to Version 3.0

The *TerminusType* character of the *GlacType* attribute was coded following Paul et al. (2009), with the addition of code 5 for shelf-terminating glaciers. Classification was done visually using imagery from a variety of sources. In a few instances, more than one terminus type applied to a particular glacier. Each such glacier was assigned the code representing the longest part of its perimeter.

Changes from Version 1.0 to Version 2.0

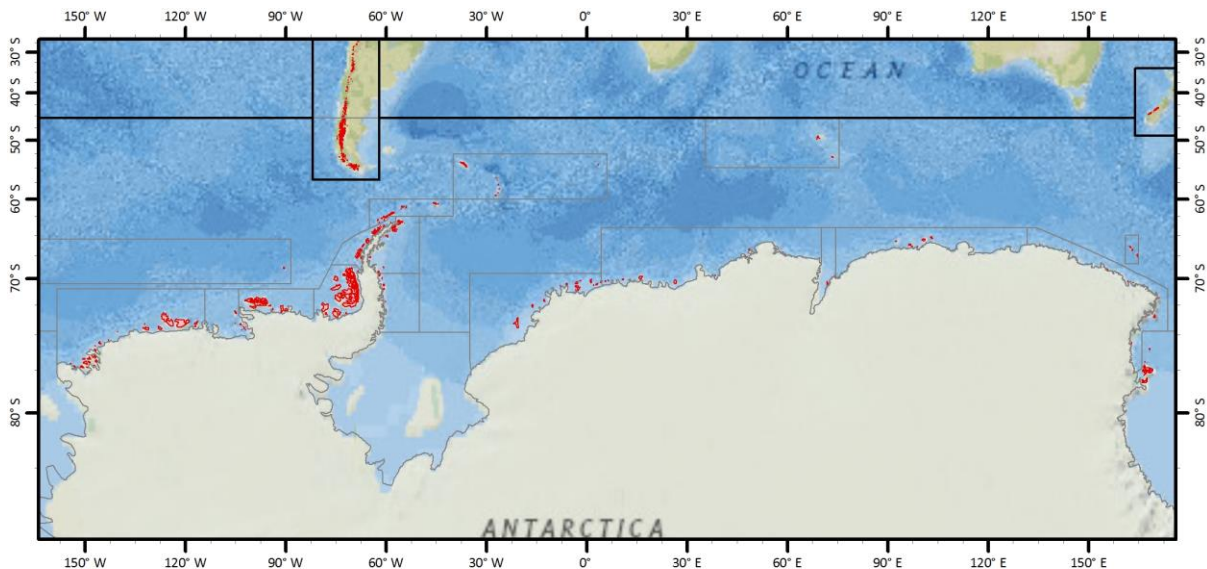
The ice cover of Peter the First Island in the Bellingshausen Sea was taken from the ADD in version 1.0. In version 2.0 it is replaced by the outlines of 26 glaciers from an inventory by J.G. Cogley (Cogley et al., 2014).

Version 1.0

Outlines of glacier complexes on islands peripheral to the mainland of Antarctica were obtained from the Antarctic Digital Database (ADD Consortium, 2000). A. Bliss manually classified the ADD's "land" polygons into continent, ice rise, ice cap, and glacier-complex polygons. Ice rises, and ice bodies on the continental mainland, are not included in this inventory. Nor are ice shelves. The classification was based on the surface morphology and surface flow velocities observed in data from Landsat, the RADARSAT Antarctic Mapping Project DEM, and the MEaSURES InSAR-based Antarctic Velocity Map. On islands with prominent nunataks, glacier complexes were subdivided into individual glaciers following Kienholz et al. (2013). More details on the processing of these outlines are given by Bliss et al. (2013).

Outlines of glaciers on most of the Subantarctic islands were obtained by E. Berthier and J.G. Cogley from various sources including satellite imagery and maps (Cogley et al., 2014). For King George Island in the South Shetland Islands, outlines were downloaded from KGIS, the King George Island Geographic Information System, a now defunct web site created by F. Rau and S. Vogt, University of Freiburg. Separate outlines of "glacier basins" and ice-free areas were harmonized and merged to form glacier outlines containing nunataks. For Kerguelen, outlines are from Berthier et al. (2009).

Outlines of South Georgia glaciers were mapped by F. Paul from a Landsat ETM+ scene from 2003 using a band 3/5 ratio and manual corrections for icebergs and water (removed), and debris-cover (added); some regions covered by seasonal snow might be included.



6 Summary of Regional Glacier Counts and Areas

The following table summarizes the number of glaciers and glacierized area of the 19 first-order regions of the RGI, version 6.0.

Region number	Region name	Glacier count	Glacierized area (km ²)
00	World	215547	705738.793
01	Alaska	27108	86725.053
02	Western Canada and US	18855	14524.224
03	Arctic Canada North	4556	105110.642
04	Arctic Canada South	7415	40888.228
05	Greenland Periphery	19306	89717.066
06	Iceland	568	11059.700
07	Svalbard	1615	33958.934
08	Scandinavia	3417	2949.103
09	Russian Arctic	1069	51591.600
10	North Asia	5151	2410.051
11	Central Europe	3927	2092.146
12	Caucasus and Middle East	1888	1306.992
13	Central Asia	54429	49303.415
14	South Asia West	27988	33568.298
15	South Asia East	13119	14734.204
16	Low Latitudes	2939	2341.036
17	Southern Andes	15908	29429.080
18	New Zealand	3537	1161.801
19	Antarctic and Subantarctic	2752	132867.220

7 References

- ADD Consortium, 2000, *Antarctic Digital Database, Version 3.0, Database, Manual and Bibliography*. Scientific Committee on Antarctic Research, Cambridge. 93p and digital data (version 4.1; <http://www.scar.org/data-products/add>).
- Andreassen, L.M., S.H. Winsvold, (Eds), F. Paul, and J.E. Hausberg, 2012, Inventory of Norwegian Glaciers. *NVE Report 28*, 236 pp. http://publikasjoner.nve.no/rapport/2012/rapport2012_38.pdf
- Andreassen, L.M., F. Paul, A. Kääh, and J.E. Hausberg, 2008, Landsat-derived glacier inventory for Jotunheimen, Norway, and deduced glacier changes since the 1930s, *The Cryosphere*, **2**, 131-145. <http://dx.doi.org/10.5194/tc-2-131-2008>.
- Beedle, M., M. Dyurgerov, W. Tangborn, S. Khalsa, C. Helm, B. Raup, R. Armstrong, and R. Barry, 2008, Improving estimation of glacier volume change: a GLIMS case study of Bering Glacier System, Alaska, *The Cryosphere*, **2**, 33-51. <http://dx.doi.org/10.5194/tc-2-33-2008>.
- Berthier, E., R. Le Bris, L. Mabileau, L. Testut, and F. Rémy, 2009, Ice wastage on the Kerguelen Islands(49S, 69E) between 1963 and 2006, *Journal of Geophysical Research*, **114**(F3). <http://dx.doi.org/10.1029/2008JF001192>.
- Berthier, E., E. Schiefer, G. Clarke, B. Menounos, and F. Rémy, 2010, Contribution of Alaskan glaciers to sea level rise derived from satellite imagery, *Nature Geoscience*, **3**, 92-95. <http://dx.doi.org/10.1038/ngeo737>.
- Bhambri, R., T. Bolch, P. Kawishwar, D.P. Dobhal, D. Srivastava and B. Pratap, 2013, Heterogeneity in glacier response in the upper Shyok valley, northeast Karakoram, *The Cryosphere*, **7**, 1385-1398. <http://dx.doi.org/10.5194/tc-7-1385-2013>.
- Björnsson, H., F. Pálsson, O. Sigurðsson and G.E. Flowers, 2003, Surges of glaciers in Iceland, *Annals of Glaciology*, **36**, 82-90.
- Bliss, A., R. Hock and J.G. Cogley, 2013, A new inventory of mountain glaciers and ice caps for the Antarctic periphery, *Annals of Glaciology*, **54**(63), 191-199.
- Bolch, T., 2007, Climate change and glacier retreat in northern Tien Shan (Kazakhstan/Kyrgyzstan) using remote sensing data, *Global and Planetary Change*, **56**, 1-12. <http://dx.doi.org/10.1016/j.gloplacha.2006.07.009>.
- Bolch, T., B. Menounos, and R.D. Wheate, 2010a, Landsat-based inventory of glaciers in western Canada, 1985-2005, *Remote Sensing of Environment*, **114**(1), 127-137. doi: <http://dx.doi.org/10.1016/j.rse.2009.08.015>.
- Bolch, T., T. Yao, S. Kang, M.F. Buchroithner, D. Scherer, F. Maussion, E. Huintjes, and C. Schneider, 2010b, A glacier inventory for the western Nyainqentanglha Range and Nam Co Basin, Tibet, and glacier changes 1976-2009, *The Cryosphere*, **4**, 419-433. <http://dx.doi.org/10.5194/tc-4-419-2010>.
- Burgess, E.W., R.R. Forster and C.F. Larsen, 2013, Summer melt regulates winter glacier flow speeds throughout Alaska, *Nature Communications*, **40**(23), 6160-6164. <http://dx.doi.org/10.1002/2013GL058228>.
- Clarke, G.K.C., J.P. Schmok, C.S.L. Ommanney and S.G. Collins, 1986, Characteristics of surge-type glaciers, *Journal of Geophysical Research*, **91**(B7), 7165-7180. <http://dx.doi.org/10.1029/JB091iB07p07165>.
- Cogley, J.G., 2009, A more complete version of the World Glacier Inventory, *Annals of Glaciology*, **50**(53), 32-38.
- Cogley, J.G., E. Berthier and S. Donoghue, 2014, Remote sensing of glaciers of the Subantarctic islands, in Kargel, J.S., M.P. Bishop, A. Kääh, B. Raup and G. Leonard, eds., *Global Land Ice Measurements from Space: Satellite Multispectral Imaging of Glaciers*, 759-780. Praxis-Springer.

- Copland, L., M.J. Sharp and J.A. Dowdeswell, 2003, The distribution and flow characteristics of surge-type glaciers in the Canadian High Arctic, *Annals of Glaciology*, **36**, 73-81.
- Copland, L., T. Sylvestre, M.P. Bishop, J.F. Shroder, Y.B. Seong, L.A. Owen, A. Bush and U. Kamp, 2011, Expanded and recently increased glacier surging in the Karakoram, *Arctic, Antarctic, and Alpine Research*, **43**(4), 503-516. <http://dx.doi.org/10.1657/1938-4246-43.4.503>.
- Chinn, T.J., 2001, Distribution of the glacial water resources of New Zealand, *Journal of Hydrology, New Zealand*, **40**(2), 139-187.
- Citterio, M., F. Paul, A.P. Ahlstrøm, H.F. Jepsen, and A. Weidick, 2009, Remote sensing of glacier change in West Greenland: accounting for the occurrence of surge-type glaciers, *Annals of Glaciology*, **50**(53), 70-80. <http://dx.doi.org/10.3189/172756410790595813>.
- Danko, D.M., 1992, The digital chart of the world project, *Photogrammetric Engineering and Remote Sensing*, **58**(8), 1125-1128.
- De Angelis, H., 2014, Hypsometry and sensitivity of the mass balance to changes in equilibrium-line altitude: the case of the Southern Patagonia Icefield, *Journal of Glaciology*, **60**(219), 14-28.
- Earl, L., and A.S. Gardner, 2016, A satellite-derived glacier inventory for North Asia, *Annals of Glaciology*, **57**(71), 50-60.
- Fountain, A.G., M. Hoffman, K. Jackson, H. Basagic, T. Nylén and D. Percy, 2007, Digital outlines and topography of the glaciers of the American West, *Open-File Report 2006-1340*, U.S. Geological Survey, 23p.
- Frey, H., F. Paul, and T. Strozzi, 2012, Compilation of a glacier inventory for the western Himalayas from satellite data: methods, challenges and results, *Remote Sensing of Environment*, **124**, 832-843. <http://dx.doi.org/10.1016/j.rse.2012.06.020>.
- Gardent, M., A. Rabatel, J.-P. Dedieu and P. Deline, 2014, Multitemporal glacier inventory in the French Alps from the late 1960s to the late 2000s, *Global and Planetary Change*, **120**, 24-37. <https://dx.doi.org/10.1016/j.gloplacha.2014.05.004>.
- Gardner, A.S., G. Moholdt, J.G. Cogley, B. Wouters, A.A. Arendt, J. Wahr, E. Berthier, R. Hock, W.T. Pfeffer, G. Kaser, S.R.M. Ligtenberg, T. Bolch, M.J. Sharp, J.O. Hagen, M.R. van den Broeke and F. Paul, 2013, A consensus estimate of glacier contributions to sea level rise: 2003 to 2009, *Science*, **340**, 852-857.
- Gellatly, A.F., C. Smiraglia, J.M. Grove and R. Latham, 1994a, Recent variations of Ghiacciaio del Calderone, Abruzzi, Italy, *Journal of Glaciology*, **40**(136), 486-490.
- Gellatly, A.F., J.M. Grove, R. Latham and R.J. Parkinson, 1994b, Observations of the glaciers in the southern Maritime Alps (Italy), *Revue de Géomorphologie Dynamique*, **43**(3), 93-107.
- Grunewald, K., C. Weber, J. Scheithauer and F. Haubold, F., 2006, Mikrogletscher im Piringebirge (Bulgarien), *Zeitschrift für Gletscherkunde und Glazialmorphologie*, **39**, 99-114.
- Guo, W.Q., S.Y. Liu, J.L. Xu, L.Z. Wu, D.H. Shangguan, X.J. Yao, J.F. Wei, W.J. Bao, P.C. Yu, Q. Liu and Z.L. Jiang, 2015, The second Chinese glacier inventory: data, methods and results, *Journal of Glaciology*, **61**(226), 357-372. <http://dx.doi.org/10.3189/2015JoG14J209>.
- Haerberli, W., M. Hoelzle, and S. Suter, eds., 1998, *Into the Second Century of World-Wide Glacier Monitoring – Prospects and Strategies*, UNESCO, Paris.
- Hagg, W., C. Mayer, E. Mayr and A. Heilig, 2012, Climate and glacier fluctuations in the Bavarian Alps in the past 120 years, *Erdkunde*, **66**(2), 121-142.
- Hagen, J.O., O. Liestøl, E. Roland, and T. Jørgensen, 1993, Glacier Atlas of Svalbard and Jan Mayen, *Norsk Polarinstitutt Meddelelser*, **129**, Oslo. 141p., 17 maps.
- Hoffman, M.J., A.G. Fountain and J.M. Achuff, 2007, 20th-century variations in area of cirque glaciers and glacierets, Rocky Mountain National Park, Rocky Mountains, Colorado, USA, *Annals of Glaciology*, **46**, 349-354.

- Howat, I.M., A. Negrete and B.E. Smith, 2014, The Greenland Ice Mapping Project (GIMP) land classification and surface elevation datasets, *The Cryosphere*, **8**, 1509-1518.
<http://dx.doi.org/10.5194/tc-8-1509-2014>.
- Hughes, P.D., 2008, Response of a Montenegro glacier to extreme summer heatwaves in 2003 and 2007, *Geografiska Annaler*, **90A**(4), 259-267.
- Huss, M., and D. Farinotti, 2012, Distributed ice thickness and volume of all glaciers around the globe, *Journal of Geophysical Research*, **117**, F04010.
<http://dx.doi.org/10.1029/2012JF002523>.
- ICIMOD, 2011a, *Glacial Lakes and Glacial Lake Outburst Floods in Nepal – Additional Material*. International Centre for Integrated Mountain Development, Kathmandu, 2011. DVD, report, data.
- ICIMOD, 2011b, *The Status of Glaciers in the Hindu Kush-Himalayan Region*, Bajracharya, S.R., and B. Shrestha, eds., International Centre for Integrated Mountain Development, Kathmandu, Nepal.
- Jordan, E., L. Ungerechts, B. Cáceres, A. Peñafiel and B. Francou, 2005, Estimation by photogrammetry of the glacier recession on the Cotopaxi Volcano (Ecuador) between 1956 and 1997, *Hydrological Sciences Journal*, **50**(6), 949-961.
<http://dx.doi.org/10.1623/hysj.2005.50.6.949>.
- Kienholz, C., S. Herreid, J.L. Rich, A.A. Arendt, R. Hock and E.W. Burgess, 2015, Derivation and analysis of a complete modern-date glacier inventory for Alaska and northwest Canada, *Journal of Glaciology*, **61**(227), 403-420. <http://dx.doi.org/10.3189/2015JoG14J230>.
- Kienholz, C., J.L. Rich, A.A. Arendt and R. Hock, 2014, A new method for deriving glacier centerlines applied to glaciers in Alaska and northwest Canada, *The Cryosphere*, **8**, 503–519.
<http://dx.doi.org/10.5194/tc-8-503-2014>.
- Kienholz, C., R. Hock and A. Arendt, 2013, A new semi-automatic approach for dividing glacier complexes into individual glaciers, *Journal of Glaciology*, **59**(217), 925-937.
<http://dx.doi.org/10.3189/2013JoG12J138>.
- König, M., C. Nuth, J. Kohler, G. Moholdt and R. Pettersen, 2013, A digital glacier database for Svalbard, in Kargel, J.S., M.P. Bishop, A. Käab, B. Raup and G. Leonard, eds., *Global Land Ice Measurements from Space: Satellite Multispectral Imaging of Glaciers*, Praxis-Springer, in press.
- Korona, J., Berthier, E., Bernard, M., Remy, F., and Thouvenot, E.: SPIRIT. SPOT 5 stereoscopic survey of Polar Ice, 2009, Reference Images and Topographies during the fourth International Polar Year (2007-2009), *ISPRS Journal of Photogrammetry and Remote Sensing*, **64**, 204-212.
<https://doi.org/10.1016/j.isprsjprs.2008.10.005>.
- Kriegel, D., C. Mayer, W. Hagg, S. Vorogushyn, D. Duethmann, A. Gafurov and D. Farinotti, 2013, Changes in glacierisation, climate and runoff in the second half of the 20th century in the Naryn basin, Central Asia, *Global and Planetary Change*, **110**, 51–61.
<http://dx.doi.org/10.1016/j.gloplacha.2013.05.014>.
- Kutuzov, S., and M. Shahgedanova, 2009, Glacier retreat and climatic variability in the eastern Terske-Alatoo, inner Tien Shan between the middle of the 19th century and beginning of the 21st century, *Global and Planetary Change*, **69**(1-2), 59–70.
<http://dx.doi.org/10.1016/j.gloplacha.2009.07.001>.
- Kurter, A., 1991, Glaciers of Turkey, in Williams, R.S., Jr., and J.G. Ferrigno, eds., *Satellite Image Atlas of Glaciers of the World*, U.S. Geological Survey Professional Paper 1386-G, 1-30.
- Le Bris, R., F. Paul, H. Frey, and T. Bolch, 2011, A new satellite-derived glacier inventory for western Alaska, *Annals of Glaciology*, **52**(59), 135-143.
- Liu, H., K. Jezek, B. Li, and Z. Zhao, 2001, *Radarsat Antarctic Mapping Project digital elevation model version 2*. Boulder, CO: National Snow and Ice Data Center. Digital media.

- Machguth, H., and M. Huss, 2014, The length of the world's glaciers – a new approach for the global calculation of center lines, *The Cryosphere*, **8**, 1741–1755. <https://doi.org/10.5194/tc-8-1741-2014>.
- Milivojević, M., L. Menković and J. Čalić, 2008, Pleistocene glacial relief of the central part of Mt. Prokletije (Albanian Alps), *Quaternary International*, **190**, 112–122. <http://dx.doi.org/10.1016/j.quaint.2008.04.006>.
- Moholdt, G., B. Wouters and A.S. Gardner, 2012, Recent mass changes of glaciers in the Russian High Arctic, *Geophysical Research Letters*, **39**, L10502. <http://dx.doi.org/10.1029/2012GL051466>.
- Mool, P.K., S.R. Bajracharya, B. Shrestha, S.P. Joshi, K. Shakya, A. Baidya and G.S. Dangol, 2007, *Inventory of Glaciers, Glacial Lakes and the Identification of Potential Glacial Lake Outburst Floods (GLOFs) Affected by Global Warming in the Mountains of Himalayan Region*. International Centre for Integrated Mountain Development, Kathmandu. DVD, report, data.
- Mool, P.K., S.R. Bajracharya, B. Shrestha, S.P. Joshi, R. Roohi, A. Arshad, R. Naz, S.A. Hussain and M.H. Chaudhry, 2005, *Indus Basin: Inventory of Glaciers and Glacial Lakes and Identification of Potential Glacial Lake Outburst Floods (GLOFs) Affected by Global Warming in the Mountains of Himalayan Region*. International Centre for Integrated Mountain Development, Kathmandu. CD-ROM, report (321p.), data.
- Mool, P.K., and S.R. Bajracharya, 2003, *Tista Basin, Sikkim Himalaya: Inventory of Glaciers and Glacial Lakes and the Identification of Potential Glacial Lake Outburst Floods (GLOFs) Affected by Global Warming in the Mountains of Himalayan Region*. International Centre for Integrated Mountain Development, Kathmandu. CD-ROM, report (136p.), data.
- Mool, P.K., D. Wangda, S.R. Bajracharya, K.Kunzang, D.R. Gurung and S.P. Joshi, 2001, *Inventory of Glaciers, Glacial Lakes and Glacial Lake Outburst Floods – Monitoring and Early Warning Systems in the Hindu Kush-Himalayan Region: Bhutan*. International Centre for Integrated Mountain Development, Kathmandu. CD-ROM, report (127p.), data.
- Morin, P., C. Porter, M. Cloutier, I. Howat, M.-J. Noh, M. Willis, W. Kramer, G. Bauer, B. Bates and C. Williamson, 2017, High resolution topography of polar regions from commercial satellite imagery, petascale computing and open source software, *Geophysical Research Abstracts*, **19**, EGU2017-3648.
- Moussavi, M.S., M.J. Valadan Zoej, F. Vaziri, M.R. Sahebi and Y. Rezaei, 2009, A new glacier inventory of Iran, *Annals of Glaciology*, **50**(53), 93-103.
- Müller, F., T. Caflisch and G. Müller, 1978, *Instructions for Compilation and Assemblage of Data for a World Glacier Inventory. Supplement: Identification/Glacier Number*. Temporary Technical Secretariat for World Glacier Inventory, Department of Geography, Federal Institute of Technology, Zürich.
- Nuimura, T., A. Sakai, K. Taniguchi, H. Nagai, D. Lamsal, S. Tsutaki, A. Kozawa, Y. Hoshina, S. Takenaka, S. Omiya, K. Tsunematsu, P. Tshering and K. Fujita, 2015, The GAMDAM glacier inventory: a quality-controlled inventory of Asian glaciers, *The Cryosphere*, **9**(3), 849–864. <http://dx.doi.org/10.5194/tc-9-849-2015>.
- Nuth, C., J. Kohler, M. König, A. von Deschwanden, J. O. Hagen, A. Käab, G. Moholdt and R. Pettersson, 2013, Decadal changes from a multi-temporal glacier inventory of Svalbard. *The Cryosphere*, **7**, 1603-1621. <http://dx.doi.org/10.5194/tc-7-1603-2013>.
- Ohmura, A., 2009, Completing the World Glacier Inventory, *Annals of Glaciology*, **50**(53), 144-148.
- Osipova, G.B., D.G. Tsvetkov, A.S. Shchetinnikov and M.S. Rudak, 1998, Katalog pul'siruyushchikh lednikov Pamira, *Materialy Glyatsiologicheskikh Issledovaniy*, **85**, 3-136.
- Osmonov, A., T. Bolch, C. Xi, A. Kurban and W.Q. Guo, 2013, Glacier characteristics and changes in the Sary-Jaz River Basin (Central Tien Shan) – 1990-2010, *Remote Sensing Letters*, **4**(8), 725–734. <http://dx.doi.org/10.1080/2150704X.2013.789146>.
- Paul, F. and N. Mölg, 2014, Hasty retreat of glaciers in northern Patagonia from 1985 to 2011. *Journal of Glaciology*, **60** (224), 1033-1043. <http://dx.doi.org/10.3189/2014JG14J104>.

- Paul, F., L.M. Andreassen, and S.H. Winsvold, 2011a, A new glacier inventory for the Jostedalbreen region, Norway, from Landsat TM scenes of 2006 and changes since 1966, *Annals of Glaciology*, **52**(59), 153-162.
- Paul, F., H. Frey, and R. Le Bris, 2011b, A new glacier inventory for the European Alps from Landsat TM scenes of 2003: challenges and results, *Annals of Glaciology*, **52**(59), 144-152.
- Paul, F. and L.M. Andreassen, 2009, A new glacier inventory for the Svartisen region, Norway, from Landsat ETM+ data: challenges and change assessment, *Journal of Glaciology*, **55**(192), 607-618.
- Paul, F., R.G. Barry, J.G. Cogley, H. Frey, W. Haeberli, A. Ohmura, C.S.L. Ommanney, B. Raup, A. Rivera, M. Zemp, 2009, Recommendations for the compilation of glacier inventory data from digital sources, *Annals of Glaciology*, **50**(53), 119-126.
- Paul, F. and A. Kääh, 2005, Perspectives on the production of a glacier inventory from multispectral satellite data in the Canadian Arctic: Cumberland Peninsula, Baffin Island, *Annals of Glaciology*, **42**, 59-66.
- Pfeffer, W.T., A.A. Arendt, A. Bliss, T. Bolch, J.G. Cogley, A.S. Gardner, J.-O. Hagen, R. Hock, G. Kaser, C. Kienholz, E.S. Miles, G. Moholdt, N. Mölg, F. Paul, V. Radić, P. Rastner, B.H. Raup, J. Rich, M.J. Sharp and the Randolph Consortium, 2014, The Randolph Glacier Inventory: a globally complete inventory of glaciers, *Journal of Glaciology*, **60**(221), 522-537..
- Raup, B., A. Kääh, J.S. Kargel, M. P. Bishop, G. Hamilton, E. Lee, F. Paul, F. Rau, D. Soltesz, S.J. Khalsa, et al., 2007, Remote sensing and GIS technology in the Global Land Ice Measurements from Space (GLIMS) project, *Computers and Geosciences*, **33**(1), 104-125.
<http://dx.doi.org/10.1016/j.cageo.2006.05.015>.
- Raup, B., and S.J. Singh Khalsa, 2007, *GLIMS Analysis Tutorial*,
<http://www.glims.org/MapsAndDocs/guides.html>. 15p.
- Raup, B., H. Kieffer, T. Hare, and J. Kargel, 2000, Generation of data acquisition requests for the ASTER satellite instrument for monitoring a globally distributed target: Glaciers, *IEEE Transactions on Geoscience and Remote Sensing*, **38**, 1105-1112.
<http://dx.doi.org/10.1109/36.841989>.
- Rignot, E., J. Mouginot, and B. Scheuchl, 2011, Ice flow of the Antarctic Ice Sheet, *Science*, **333**(6048), 1427-1430. <http://dx.doi.org/10.1126/science.1208336>.
- Rivera, A., T. Benham, G. Casassa, J. Bamber and J.A. Dowdeswell, 2007, Ice elevation and areal changes of glaciers from the Northern Patagonia Icefield, Chile, *Global and Planetary Change*, **59**, 126-137. <http://dx.doi.org/10.1016/j.gloplacha.2006.11.037>.
- Sah, M., G. Philip, P.K. Mool, S. Bajracharya and B. Shrestha, 2005, *Uttaranchal Himalaya India: Inventory of Glaciers and Glacial Lakes and the Identification of Potential Glacial Lake Outburst Floods (GLOFs) Affected by Global Warming in the Mountains of Himalayan Region*. International Centre for Integrated Mountain Development, Kathmandu. CD-ROM, report (176p.), data.
- Sarıkaya, M.A., and A.E. Tekeli, 2013, Satellite inventory of glaciers in Turkey, in Kargel, J.S., M.P. Bishop, A. Kääh, B. Raup and G. Leonard, eds., *Global Land Ice Measurements from Space: Satellite Multispectral Imaging of Glaciers*, 465-480. Praxis-Springer.
- Sedov, R.V., 1997, Ledniki Chukotki, *Materialy Glyatsiologicheskikh Issledovaniy*, **82**, 213-217.
- Sevestre, H., and D.I. Benn, 2015, Climatic and geometric controls on the global distribution of surge-type glaciers: implications for a unifying model of surging, *Journal of Glaciology*, **61**(226), 646-662.
- Shahgedanova, M., G. Nosenko, S. Kutuzov, O. Rototaeva and T. Khromova, 2014, Deglaciation of the Caucasus Mountains, Russia/Georgia, in the 21st century observed with ASTER satellite imagery and aerial photography, *The Cryosphere Discussions*, **8**, 4159-4194.
<http://dx.doi.org/10.5194/tcd-8-4159-2014>.

- Shi, Y.F., C.H. Liu, and E.S. Kang, 2009, The Glacier Inventory of China, *Annals of Glaciology*, **50**(53), 1-4.
- Shroder, J.F., Jr., and M.P. Bishop, 2010, Selected glaciers of Afghanistan, in Williams, R.S., Jr., and J.G. Ferrigno, eds., *Satellite Image Atlas of Glaciers of the World – Asia*, U.S. Geological Survey Professional Paper 1386-F, 167-199. U.S. Government Printing Office, Washington, D.C.
- Smiraglia, C., R.S. Azzoni, C. D'Agata, D. Maragno, D. Fugazza and G.A. Diolaiuti, 2015, The evolution of the Italian glaciers from the previous data base to the new Italian inventory. Preliminary considerations and results, *Geografia Fisica e Dinamica Quaternaria*, **38**, 79-87.
- Svoboda, F. and F. Paul, 2009, A new glacier inventory on southern Baffin Island, Canada, from ASTER data: I. Applied methods, challenges and solutions, *Annals of Glaciology*, **50**(53), 11-21.
- Triglav Čekada, M., M. Zorn, V. Kaufmann and G.K. Lieb, 2012, Measurements of small alpine glaciers: examples from Slovenia and Austria, *Geodetski Vestnik*, **56**(3), 462-481.,
- Way, R.G., T. Bell and N.E. Barrand, 2014, An inventory and topographic analysis of glaciers in the Torngat Mountains, northern Labrador, Canada, *Journal of Glaciology*, **60**(223), 945-956.
- WGMS, 1989, *World Glacier Inventory – Status 1988*, Haeberli, W., H. Bösch, K. Scherler, G. Østrem and C.C. Wallén, eds., IAHS (ICS) / UNEP / UNESCO, World Glacier Monitoring Service, Zürich, Switzerland. 458 p.
- White, S.E., 2002, Glaciers of Mexico, in Williams, R.S., Jr., and J.G. Ferrigno, eds., *Satellite Image Atlas of Glaciers of the World – North America*. U.S. Geological Survey Professional Paper 1386-J, 383-405. U.S. Government Printing Office, Washington, D.C.
- Wu, L.Z., T. Che, R. Jin. X. Li, T.L. Gong, Y.H. Xie, G.A. Tang, Y.M. Liu, P.K. Mool, S.R. Bajracharya, K. Shakya and G.S. Dangol, 2004, *Poiqu (Bhote-Sun Koshi) and Rongxer (Tama Koshi) Basins, Tibet Autonomous Region, PR China: Inventory of Glaciers and Glacial Lakes and the Identification of Potential Glacial Lake Outburst Floods (GLOFs) Affected by Global Warming in the Mountains of Himalayan Region*. International Centre for Integrated Mountain Development, Kathmandu. CD-ROM, report (128p.), data.
- Wu, L.Z., T. Che, R. Jin. X. Li, T.L. Gong, Y.H. Xie, P.K. Mool and S.R. Bajracharya, 2003, *Pumqu Basin, Tibet Autonomous Region of PR China: Inventory of Glaciers and Glacial Lakes and the Identification of Potential Glacial Lake Outburst Floods (GLOFs) Affected by Global Warming in the Mountains of Himalayan Region*. International Centre for Integrated Mountain Development, Kathmandu. CD-ROM, report (149p.), data.